Visualization of vitamin A metabolism

Koenders, S.T.A.

Chapter 7

Synthesis and Biological Evaluation of Clickable Vitamin A

Introduction

The functionalization of endogenous lipids with a ligation handle is commonly used for the visualization of lipid metabolism and its localization within the cell.[1] Examples that can be found in the literature include fatty acids and cholesterol.[2–7] So far this approach has not been applied to vitamin A, possibly due to a lack of efficient synthetic approaches for the facile introduction of a ligation handle.

The chemical method introduced in **Chapter 3** was used to make retinal-based probe **LEI-945**, suitable for activity-based protein profiling (ABPP).[8] This method also enables the synthesis of retinoid analogues containing an alkyne click handle starting from the key Wittig salt **1**. Such analogues can be used to study the intracellular localization of vitamin A or the exchange of retinoic acid (RA) between different cells of the immune system, which is thought to be essential for immune homeostasis.[9,10]

Clickable vitamin A analogues can also be used in affinity-based protein profiling (A_fBPP) to identify its interaction partners. Photoaffinity labelling normally requires the introduction of a photocrosslinking group, such as a diazirine[11], but retinoids are inherently photoreactive. Under the influence of visible light photoisomerization can occur[12], which is an essential reaction in the visual cycle.[13] UV light is capable of exciting non-binding electrons within the conjugated retinoid system, which can lead to radical formation.[14,15] These radicals can react with a protein interaction partner to form a covalent adduct.[16] Previously, radiolabelled retinoids have been used for the UV-induced labelling of retinoid-binding proteins, such as albumin, the cellular retinoic acid-binding protein (CRABP) and the retinoid X receptor β (RXRβ).[17–19]

In this chapter, the inherent photocrosslinking ability of clickable retinoids was employed in chemical proteomics approaches to circumvent the use of radioactive compounds.

Results and discussion

Synthesis of clickable retinoid analogues

The clickable retinoid analogues **STA-211** and **STA-215** were synthesized using the convergent synthesis route introduced in **Chapter 3**. Wittig salt **1** was coupled with aldehyde **2** to make the protected retinal analogue **STA-211** in 8% yield. Aldehyde **2** was synthesized following a literature procedure, which can be found in **Supplementary scheme 7.1**.[20] The final product was obtained in poor yield due to several purification steps, which were required to separate the product from the unreacted aldehyde **2**.

RA analogue **STA-215** was made in a similar fashion starting from Wittig salt **1** and commercially available aldehyde **3**. Compound **4** was treated with 2 M NaOH in 24% yield. **STA-211** and **STA-215** were stored in ethanol at -80 °C. Exposure of **STA-211** to slightly acidic conditions using a buffer or MilliQ instantly liberates the aldehyde after which the compound can be used for biochemical experiments.

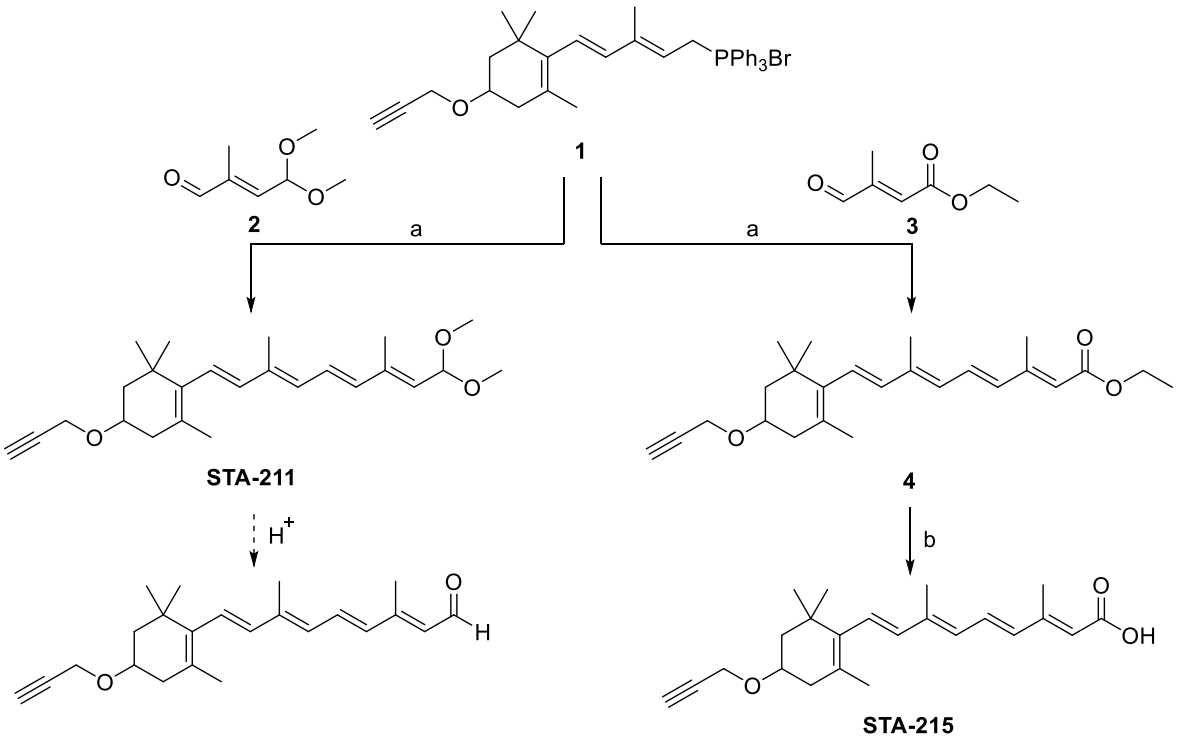

Scheme 7.1 | Synthesis of clickable vitamins. Reagents and conditions: a) *n*-BuLi, THF, -78 °C to RT, 3 h, 8% for **STA-211** and 39% for **4** (3.3:1 E/Z); b) 2 M NaOH, MeOH, 50 °C, 4 h, 24% (7:3 E/Z).

Clickable retinoic acid analogue STA-215 is biologically equivalent

To determine whether the clickable retinoic acid was biologically equivalent, its ability to differentiate human leukaemia HL60 cells was compared. HL60 cells are commonly used as a model for human myeloid cell differentiation.[21] When treated with DMSO and retinoic acid (RA) these cells differentiate into granulocytes expressing CD11b, which can be used as a biomarker for successful differentiation (**Fig. 7.1a**).[22] HL60 cells were cultured in normal RPMI growth medium or medium containing **STA-215** (1 μM), RA (1 μM), DMSO (1.25% v/v), DMSO (1.25% v/v) with **STA-215** (1 μM) and DMSO (1.25% v/v) with RA (1 μM). Cells were cultured for 72 hours, stained for CD11b and measured using fluorescence activated cell sorting (FACS). Both RA and **STA-215** on their own did not induce differentiation (**Fig. 7.1b**).

Treatment with DMSO (1.25% v/v) on its own induced granulocyte differentiation, but when combined with **STA-215** (1 μM) or RA (1 μM) the percentage of differentiated cells increased significantly with 1.5 and 2-fold, respectively. **STA-215** was able to differentiate HL60 cells in combination with DMSO into granulocytes, although to a lesser extent than RA.

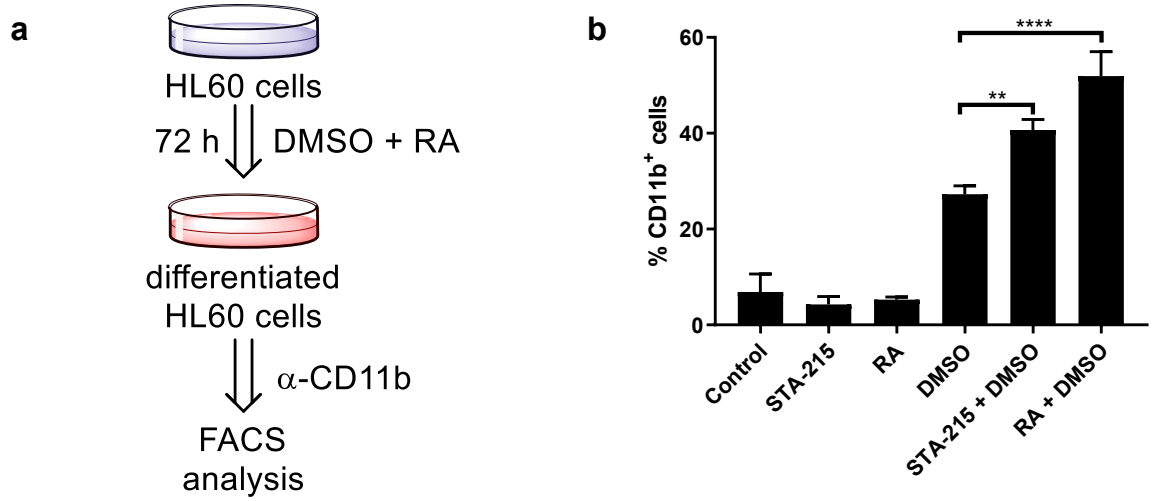

Fig. 7.1 | Validation of biological equivalence of clickable retinoic acid. a, Schematic representation of HL60 differentiation experiment. HL60 cells are treated with DMSO and retinoic acid, incubated for 72 h, stained for CD11b and analysed using FACS. **b**, Graph showing the proportion of $CD11b^+$ cells indicating the differentiation of HL60 cells into granulocytes.

To further validate whether the clickable retinoid analogues are biologically equivalent, dendritic cells were treated with **STA-211** (10 μM) or **STA-215** (10 μM) for 6 days. RA differentiated these dendritic cells, increasing aldehyde dehydrogenase (ALDH) expression in these cells as measured by the ALDEFLUOR assay (**Supplementary Fig. 7.1a**). The differentiation marker CD103 was also increased upon RA treatment (**Supplementary Fig. 7.1b**). Retinoic acid analogue **STA-215** was able to induce the same increase in ALDH activity and CD103 expression with no significant difference compared to the endogenous compound. Also between retinal and **STA-211**, no significant differences could be detected. Taken together, these data show that the clickable RA **STA-215** is capable of inducing differentiation.

Photoaffinity labelling with clickable vitamins

Having validated the biological equivalence of clickable retinoic acid, its application in a photoaffinity proteomics approach was studied. HL60 cells were treated with either **STA-211** (10 μM, 1 h) or **STA-215** (10 μM, 1 h) and irradiated for 10 minutes with UV-light (350 nm). The samples were washed, lysed, clicked and resolved by sodium dodecyl sulphate polyacrylamide gel electrophoresis (SDS-PAGE) and visualized by in-gel fluorescent scanning.

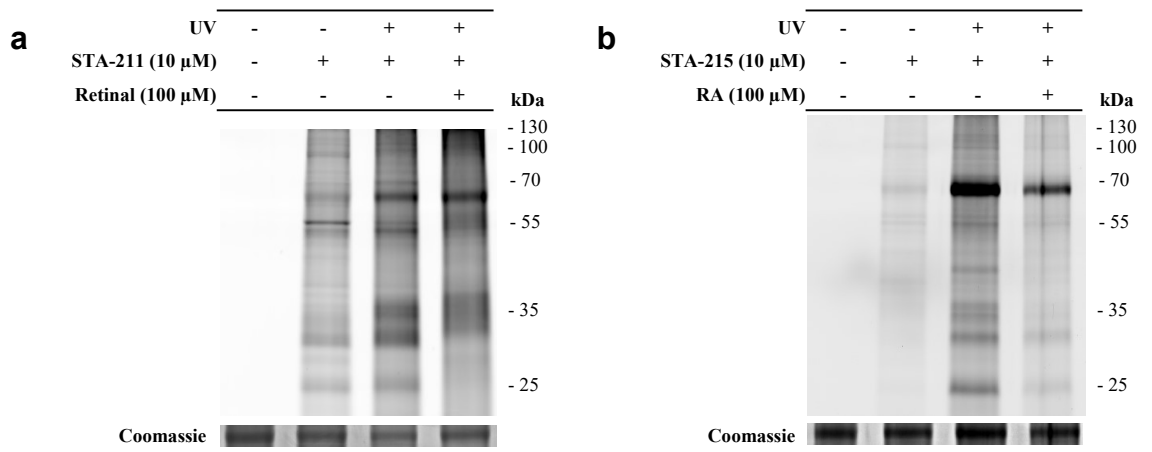

Fig. 7.2 | Validation of biological equivalence of clickable retinoic acid and photoaffinity labelling of clickable retinoids. a, Fluorescence labelling of HL60 cells treated with **STA-211** (10 µM, 1 h) and irradiated with UV-light (350 nm, 10 min). **b**, Fluorescence labelling of HL60 cells treated with **STA-215** (10 µM, 1 h) and irradiated with UV-light (350 nm, 10 min).

Cells treated with **STA-211** showed a relatively high amount of background labelling, probably due to interactions of the reactive aldehyde group with enzymes (**Fig. 7.2a**). One clear fluorescent band is visible around 55 kDa in the non-UV induced samples. Upon UV irradiation the intensity of the labelling increases, which could be partially outcompeted by retinal (100 µM).

In HL60 cells treated with **STA-215** (10 µM, 1 h) there is an increase in labelling upon UV irradiation (**Fig. 7.2b**). Around 70 kDa a prominent fluorescent band is visible. The UV-induced labelling by **STA-215** can also be competed with RA (100 µM). These data indicate that the clickable retinoid analogues can be used as photoaffinity probes. To identify the labelled proteins, **STA-215** was subjected to a chemical proteomics experiment. HL60 cells were treated as described above. Samples were ligated with biotin azide and the probe-labelled proteins subsequently enriched using avidin-beads. After several washing steps the proteins were digested on-bead using trypsin and then measured and identified using mass spectrometry. 34 Proteins were enriched by **STA-215** without UV-irradiation, including apolipoprotein A-1 (APOA1) (**Fig. 7.3a**). UV-induced labelling resulted in 192 UV-enriched proteins of which 36 could be competed away by RA (**Fig. 7.3b,c, Supplementary Table 7.1**). Interestingly, fatty acid binding protein 5 (FABP5)[23], a known RA binding protein, was not enriched by **STA-215**, while two apolipoproteins (APOA1 and APOM) and serum albumin were significantly enriched by the RA analogue.

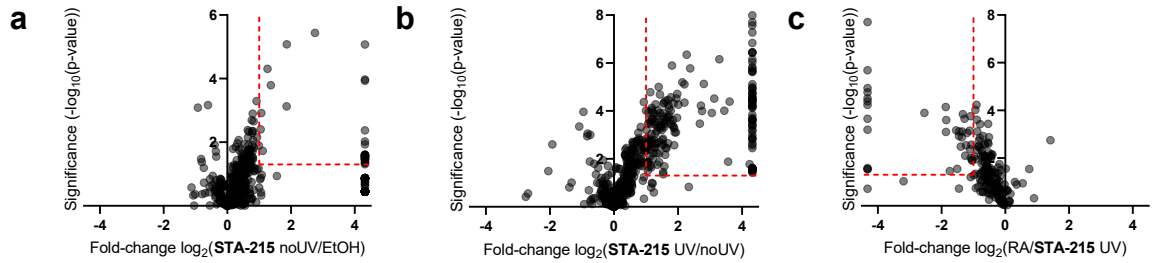

Fig. 7.3 | Photoaffinity labelling of HL60 cells with clickable retinoic acid. a, Volcano plot of total proteins identified in a chemical proteomics experiment with probe **STA-215** (10 μM). Red lines indicate threshold values (fold-change > 2; p-value < 0.05) marking significantly probe-enriched proteins. **b**, Volcano plot of total proteins identified in a chemical proteomics experiment with probe **STA-215** (10 μM). Red lines indicate threshold values (fold-change > 2; p-value < 0.05) marking significantly UV-enriched proteins. **c**, Volcano plot of UV-enriched proteins in a chemical proteomics experiment with probe **STA-215** (10 μM). Red lines indicate threshold values (fold-change < 0.5; p-value < 0.05) marking significantly competed proteins by retinoic acid (RA). For parts **a**-**c**, data are from $N = 4$ experiments (biological replicates).

Analysis of the UV-enriched proteins with DAVID[24] analytic tools using the KEGG[25] database showed a high representation of enzymes involved in protein processing. Furthermore, enzymes involved in Alzheimer's, Huntington's and Parkinson's disease were found in this group of UV-enriched enzymes (**Fig. 7.4a**). The enriched proteins annotated to this group, include the NADH:ubiquinone oxidoreductase subunits, cytochrome c oxidase subunits, solute carriers and voltage dependent anion channels. Analysis using the PANTHER[26] database indicated that the majority of UV-enriched proteins are annotated as catalytic enzymes or binding/transporter proteins. These data show that the clickable retinoic acid analogue **STA-215** can be used for the A_fBPP of retinoid-interacting proteins.

An activity-based chemical proteomics approach with the activity-based probe **LEI-945** in HL60 cells identified 231 significantly enriched proteins (**Supplementary Table 7.2**). Of these proteins, 142 were also UV-enriched by **STA-215**. 24 Proteins of this group were competed by RA in a competitive A_fBPP experiment (**Fig. 7.4c**). Only one ALDH was found in these cells, ALDH3A2. This aldehyde dehydrogenase was also UV-enriched by **STA-215** and competed by RA.

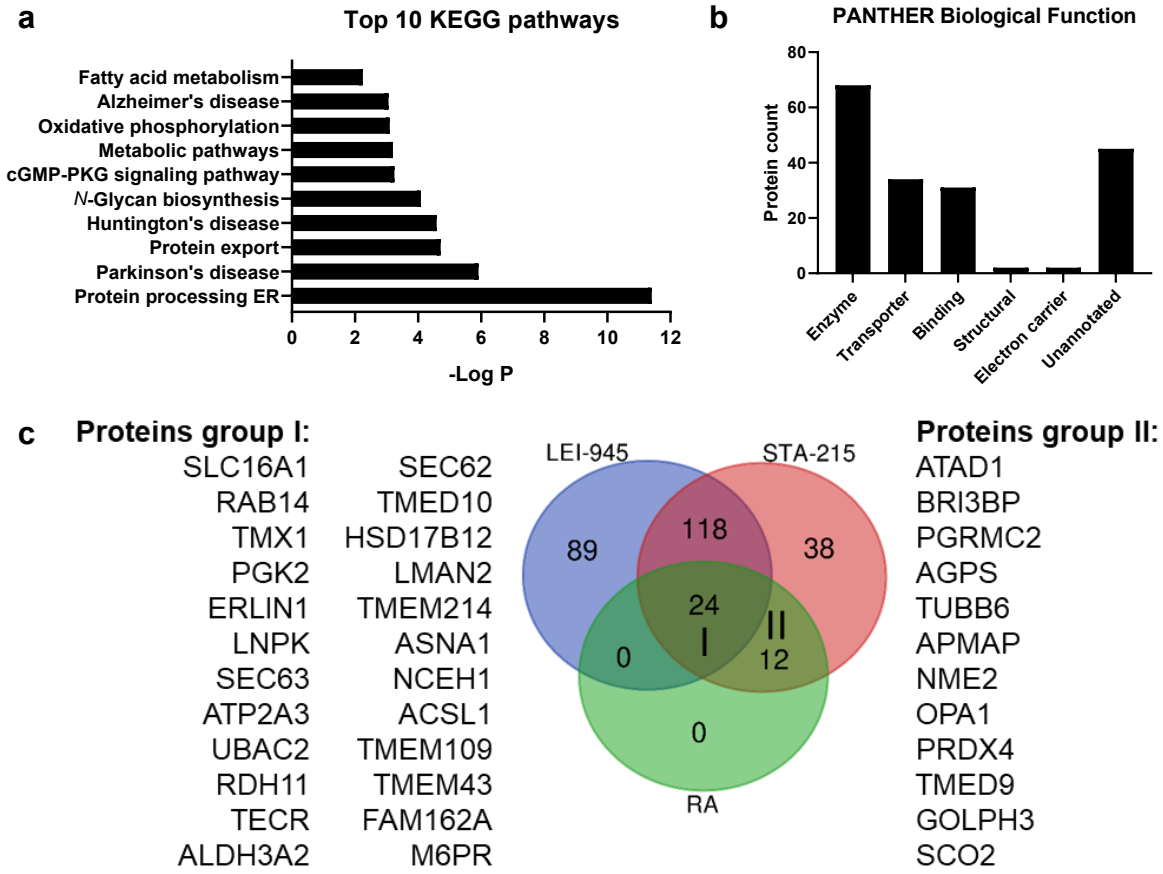

Fig. 7.4 | Proteomics data of UV-enriched proteins by STA-215 in HL60 cells and comparison with LEI-945. a, Top 10 pathways enriched in the group of significantly UV-enriched proteins as determined by screening on the KEGG database. **b**, Molecular functions attributed to significantly UV-enriched proteins by the PANTHER database. **c**, Venn diagram showing the overlap in proteins enriched by **LEI-945**, UV-enriched by **STA-215** and UV-enriched by **STA-215** and competed by retinoid acid.

Both **STA-211** and **STA-215** were then used for A_fBPP in the adherent non-small cell lung cancer cell line A549. As this cell line is capable of producing retinoic acid, it was expected that more retinoid-interacting proteins would be expressed in A549 cells. Samples from cells treated with **STA-211** (10 μM, 30 min), showed a fluorescent band around 55 kDa without UV irradiation. Upon UV-induced labelling a fluorescent band around 40 kDa was visible, which could be competed for by both retinal and retinoic acid. Cells treated with **STA-215** (10 μM, 30 min) showed a similar labelling pattern to **STA-211**, but with an extra fluorescent band appearing around 30 kDa and less prominent labelling of the proposed ALDH1A1 band around 55 kDa. Overall there was less background labelling in the samples treated with **STA-215** compared to **STA-211**, similar to the samples derived from the HL60 cells.

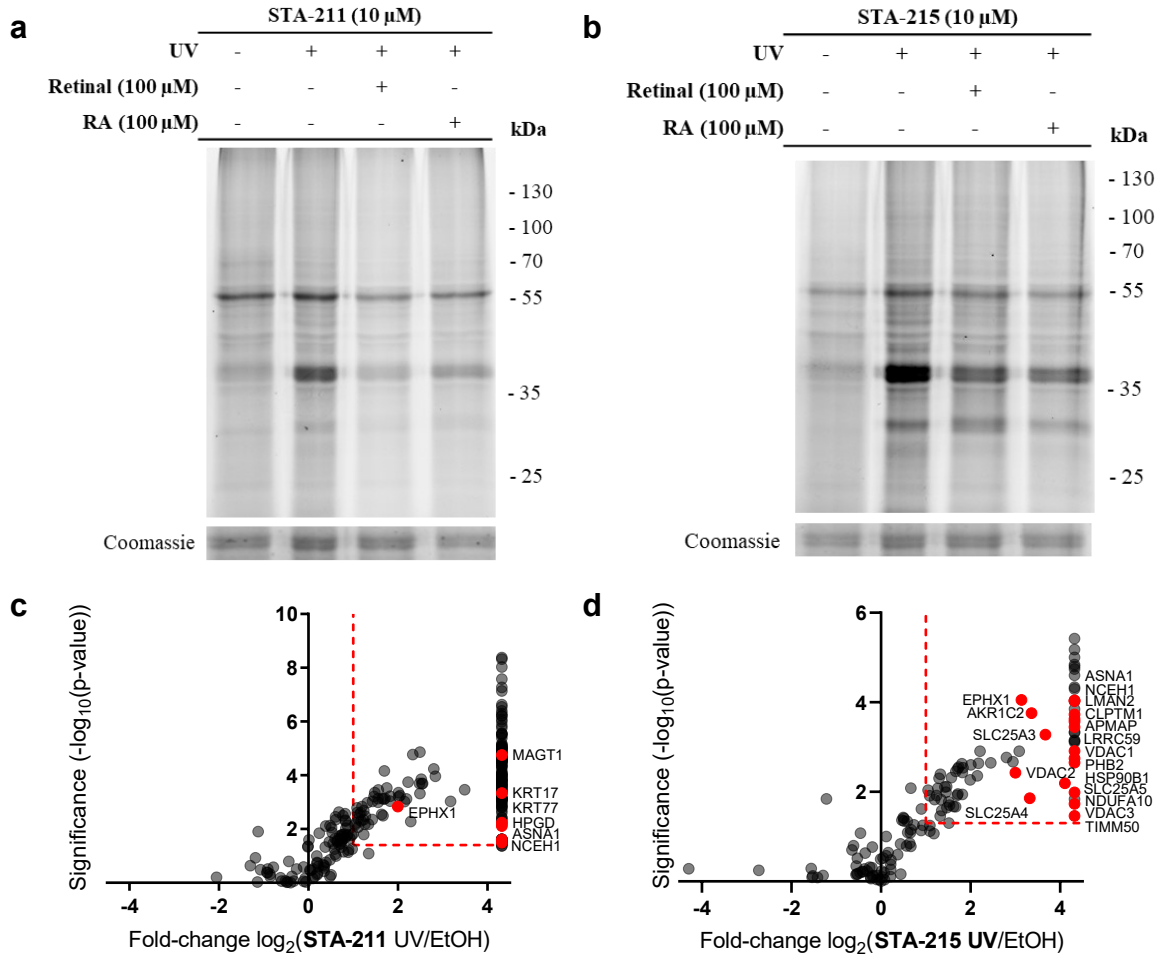

Fig. 7.5 | Photoaffinity labelling of A549 cells with clickable retinoids. a, A549 cells treated with **STA-211** (10 µM, 30 min) and irradiated on ice with UV-light (350 nm, 10 min). **b**, A549 cells treated with **STA-215** (10 µM, 30 min) and irradiated on ice with UV-light (350 nm 10 min). **c**, Volcano plot of total proteins identified in chemical proteomics experiment with probe **STA-211** (10 µM). Red lines indicate threshold values (fold-change > 2; p-value < 0.05) marking significantly enriched proteins. Red dots indicate UV-enriched proteins. Data are from $N = 4$ experiments (biological replicates). **d**, Volcano plot of total proteins identified in chemical proteomics experiment with probe **STA-215** (10 µM). Red lines indicate threshold values (fold-change > 2; p-value < 0.05) marking significantly enriched proteins. Red dots indicate UV-enriched proteins. Data are from $N = 2$ experiments (biological replicates).

The samples were then subjected to a chemical proteomics A_fBPP experiment as described previously. In correspondence with the results from the fluorescent labelling, **STA-211** significantly enriched 71 proteins without UV irradiation, whereas **STA-215** only enriched 14 proteins. Upon UV irradiation only 7 proteins were enriched by **STA-211**, however, 5 of these were only identified in the UV-enriched samples (**Fig. 7.5c**).

Of the UV-enriched proteins, 5 could be significantly competed by pretreatment with retinal (100 μM): epoxide hydrolase 1 (EPHX1), keratin (KRT17), neutral cholesterol ester hydrolase (NCEH1), ATPase (ASNA1) and magnesium transporter protein 1 (MAGT1). Although **STA-211** has high background labelling of itself, probably due to the labelling of proteins via its aldehyde, UV irradiation does expand the coverage of the retinal interacting proteins detected.

STA-215 on the other hand, UV-enriched 21 proteins (**Fig. 7.5d**), 7 of which could be competed by pretreatment with retinoic acid (100 μM), which include epoxide hydrolase 1 (EPHX1), neutral cholesterol ester hydrolase (NCEH1), ADP/ATP translocase 1 (SLC25A4), vesicular integral-membrane protein VIP36 (LMAN2), aldo-keto reductase family 1 member C2 (AKR1C2), mitochondrial phosphate carrier protein (SLC25A3) and prohibitin-2 (PHB2). An overview of the proteins enriched in these experiments can be found in **Supplementary table 7.3** and **7.4**.

In comparison with the proteins enriched by **LEI-945**, neutral cholesterol ester hydrolase 1 (NCEH1) and epoxide hydrolase 1 (EPHX1) are shared with **STA-211** and **STA-215**. Four are shared with **STA-215** alone, which are the voltage-dependent anion-selective channel protein 2 (VDAC2), voltage-dependent anion-selective channel protein 3 (VDAC3), ADP/ATP translocase 2 (ADT2) and mitochondrial phosphate carrier protein (SLC25A3).

Cellular localization of clickable vitamins using imaging flow cytometry

To determine the cellular localization of the clickable retinoids, imaging flow cytometry was used. This technique combines flow cytometry with fluorescence cell imaging, which provides spatial and morphological information in a quantitative manner.[27] A549 cells were treated with vehicle, **STA-211** (10 μM) or **STA-215** (10 μM) for 1 hour. Cells were then suspended into a single cell suspension, fixed and clicked with Alexa Fluor 488. After staining of the nucleus, cells were analysed using imaging flow cytometry. The treatment of vehicle-treated cells with the Alexa Fluor 488 “click mix” led to some background labelling, however a clear increase in fluorescence intensity could be seen in cells treated with a clickable vitamin (**Supplementary Fig. 7.2**).

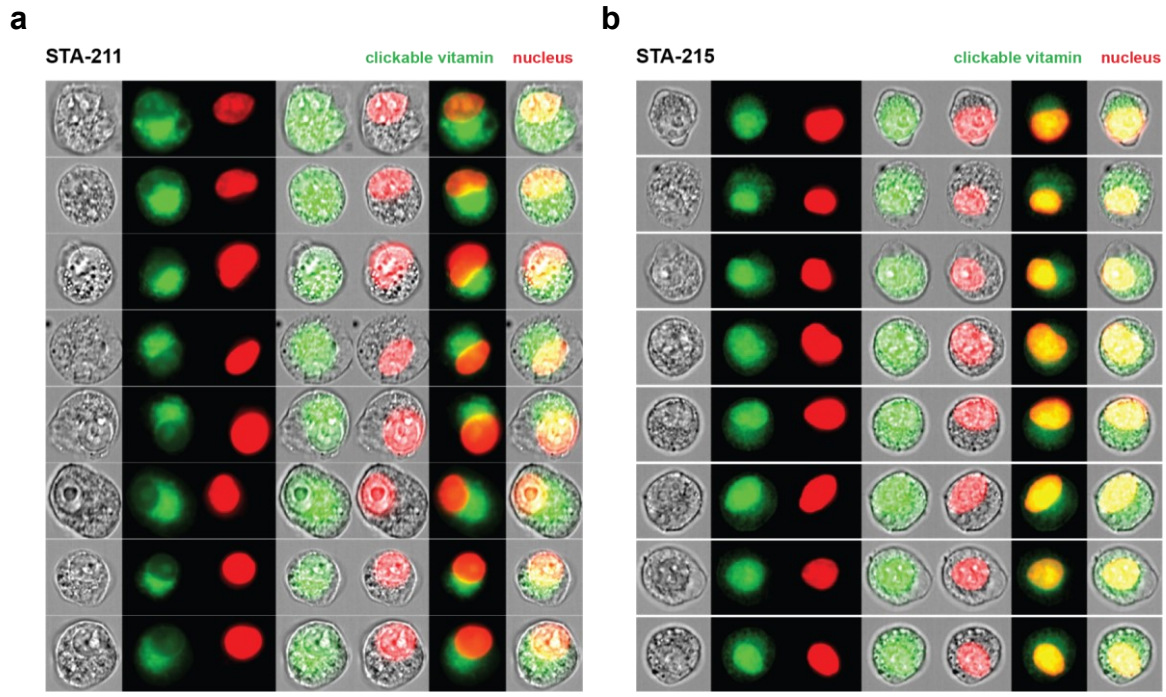

Fig. 7.6 | Localization of clickable vitamins in A549 cells using imaging flow cytometry. a, Representative images of individual cells treated with **STA-211** (10 μM) showing low colocalization. Alexa Fluor 488 fluorescence is shown in green and DAPI in red. Colocalization is visualized in yellow. **b**, Representative images of individual cells treated with **STA-215** (10 μM) showing high colocalization. Alexa Fluor 488 fluorescence is shown in green and DAPI in red. Colocalization is visualized in yellow.

Preliminary data showed localization of **STA-211** in the cytoplasm (**Fig. 7.6a**), whereas **STA-215** staining localized in the nucleus (**Fig. 7.6b**). As retinoic acid exerts its effect on gene regulation in the nucleus, this difference in localization might be explained by active transport of the clickable retinoic acid to the nucleus. These data also indicate that (imaging) flow cytometry can be used to track the exchange of retinoids between cells, which is of interest in the field of mucosal immunology as discussed in **Chapter 6**.

Conclusion

Using the chemical methods introduced in **Chapter 3**, retinal and retinoic acid analogues functionalized with a ligation handle were synthesized. The clickable retinoic acid analogue was shown to be biologically equivalent to its endogenous counterpart. Both probes were used in a chemical proteomics experiment and showed protein enrichment upon UV irradiation, validating their use as photoaffinity probes.

However, the retinal analogue **STA-211** showed high background labelling, probably due to covalent interactions its aldehyde with proteins. The retinoic acid analogue **STA-215**, on the other hand, showed low background labelling and enriched more proteins upon UV irradiation. Further validation and characterization of the enriched probe targets is required to unravel their involvement in retinoid biology.

Acknowledgements

Tom van der Wel is kindly acknowledged for his technical advice and collaboration on performing the HL60 differentiation experiment, Bogdan Florea for mass spectrometry analysis, Pasquale Putter for his collaboration on the A_fBPP in A549 cells and Martje Erkelens for performing and analysing the imaging flow cytometry.

Experimental procedures

Synthetic methods

General remarks. All reactions were performed using oven or flame-dried glassware and dry solvents. Reagents were purchased from Sigma Aldrich, Acros, Biosolve, VWR, Fluka, Fischer Scientific and Merck and used as received unless stated otherwise. Tetrahydrofuran (THF) and *N,N*-dimethylformamide (DMF) were stored over 4 Å molecular sieves before use. All moisture sensitive reactions were performed under a nitrogen atmosphere. TLC analysis was performed using Merck aluminum sheets (TLC silica gel 60/Kieselguhr F_{254}). Compounds were visualized using a solution of $KMnO_4$ (7.5 g), K_2CO_3 (50 g), 10% NaOH (6 mL) in H_2O (1L). Column chromatography was performed using Screening Device B.V. silica gel (particle size of 40 – 63 μm, pore diameter of 60 Å) with the indicated eluents. ^{1}H- and ^{13}C-NMR spectra were recorded on Bruker AV-400 (400 MHz and 101 MHz, respectively) or Bruker AV-500 MHz (500 MHz and 150 MHz, respectively) using $CDCl_3$ as solvent. Chemical shifts are reported in ppm (δ) relative to the residual solvent peak or tetramethylsilane. Coupling constants are given in Hz. High-resolution mass spectrometry (HRMS) analysis was performed with a LTQ Orbitrap mass spectrometer (Thermo Finnigan), equipped with an electrospray ion source in positive mode (source voltage 3.5 kV, sheath gas flow 10 mL/min, capillary temperature 250°C) with resolution R = 60000 at m/z 400 (mass range m/z = 150 – 2000) and dioctyl phthalate (m/z = 391.28428) as a "lock mass", or with a Synapt G2-Si (Waters), equipped with an electrospray ion source in positive mode (ESI-TOF), injection via NanoEquity system (Waters), with LeuEnk (m/z = 556.2771) as "lock mass". Eluents used: MeCN:H_2O (1:1 v/v) supplemented with 0.1% formic acid. The high-resolution mass spectrometers were calibrated prior to measurements with a calibration mixture (Thermo Finnigan). The retinoids were handled under dark conditions using amber colored flasks or aluminum foil when containing more than 3 conjugated double bonds. Retinoid intermediates were stored in the dark under nitrogen at -30 °C and final compounds as powder or as EtOH stock at -80 °C under nitrogen atmosphere. For further information on retinoid handling and storage we refer to the review from Barua and Furr[28].

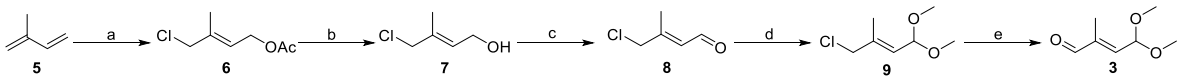

Supplementary Scheme 7.1 | Synthesis of protected aldehyde intermediate. Reagents and conditions: a) *t*BuOCl, AcOH, 1 h and then $CuSO_4$, H_2SO_4, 96 h, 30%; b) Na_2CO_3, MeOH/H_2O, 5 h, 0 °C, 33%; c) PCC, DCM, 90 min, 0 °C, 51%; d) trimethyl orthoformate, *p*TsOH, MeOH, 24 h, 67%; e) K_2HPO_4/KH_2PO_4, NaBr, DMSO, 24 h, 80 °C, 55%.

(E)-4-Chloro-3-methylbut-2-en-1-yl acetate (6):

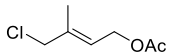

To a stirred solution of isoprene **5** (20 mL, 0.20 mol) in acetic acid (60 mL) at 0 °C under N_2 was added *tert*-butyl hypochlorite (18 mL, 0.16 mol). The reaction mixture was stirred for 1 hour and then quenched with H_2O and extracted with Et_2O. The organic layer was washed with sat. aq. $NaHCO_3$ and brine, dried with $MgSO_4$, filtered and concentrated under reduced pressure. The residue was then dissolved in acetic acid (60 mL) and to this was added $CuSO_4$ (320 mg, 2.0 mmol) and H_2SO_4 (0.2 mL, 4 mmol). The reaction mixture was stirred for 96 hours at room temperature and was then quenched with H_2O and extracted with Et_2O. The organic layer was washed with sat. aq. $NaHCO_3$ and brine, dried with $MgSO_4$, filtered and concentrated under reduced pressure. Purification of the residue by column chromatography (pentane/Et_2O) afforded the title compound **6** (7.8 g, 48 mmol, 30%). ^{1}H NMR (400 MHz, $CDCl_3$) δ 5.70 (t, J = 6.8 Hz, 1H), 4.62 (d, J = 6.9 Hz, 2H), 4.02 (s, 2H), 2.06 (s, 3H), 1.82 (s, 3H). ^{13}C NMR (101 MHz, $CDCl_3$) δ 170.4, 136.6, 123.5, 60.4, 50.5, 20.5, 14.2. Spectroscopic data for H-NMR are in agreement with those reported.[29]

(E)-4-Chloro-3-methylbut-2-en-1-ol (7):

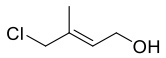

Compound **6** (7.8 g, 48 mmol) was dissolved in MeOH (120 mL). To this was added a solution of Na_2CO_3 (7.6 g, 72 mmol) in H_2O (40 mL). The reaction mixture was stirred for 5 hours at 0 °C, filtered and concentrated under reduced pressure. The remaining water layer was then extracted with $CHCl_3$. The organic layer was washed with brine, dried with $MgSO_4$, filtered and concentrated under reduced pressure. Purification of the residue by column chromatography (pentane/Et_2O) afforded the title compound **7** (1.9 g, 16 mmol, 33%). R_f (50% Et_2O in pentane) = 0.5. ^{1}H NMR (400 MHz, $CDCl_3$) δ 5.70 (s, 1H), 4.15 (s, 2H), 4.02 (s, 2H), 3.43 (s, 1H), 1.76 (s, 3H). ^{13}C NMR (101 MHz, $CDCl_3$) δ 128.8, 58.5, 51.2, 42.7, 14.1.

(E)-4-Chloro-3-methylbut-2-enal (8):

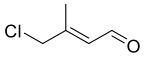

A solution of **7** (1.9 g, 16 mmol) in dry DCM (20 mL) was added to a stirred suspension of PCC (5.1 g, 24 mmol) in dry DCM (40 mL) at 0 °C under N_2 containing molecular sieves. The reaction mixture was stirred for 90 minutes at 0 °C and was then filtered over celite and concentrated under reduced pressure. Purification of the residue by column chromatography (Et_2O/pentane) afforded the title compound **8** (0.94 g, 8.0 mmol, 51%). R_f (50% Et_2O in pentane) = 0.8. ^{1}H NMR (400 MHz, $CDCl_3$) δ 10.04 (d, J = 7.7 Hz, 1H), 6.12 (d, J = 7.7 Hz, 1H), 4.12 (s, 2H), 2.28 (s, 3H); ^{13}C NMR (101 MHz, $CDCl_3$) δ 191.0, 155.2, 128.6, 49.3, 15.5.

(E)-4-Chloro-1,1-dimethoxy-3-methylbut-2-ene (9):

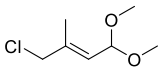

To a solution of **8** (0.94 g, 7.9 mmol) in MeOH (7 mL) was added trimethyl orthoformate (7.1 mL, 40 mmol) and *p*TsOH (0.80 mmol, 84 mg). The reaction mixture was stirred overnight at room temperature and was then quenched with sat. aq. $NaHCO_3$ and extracted with Et_2O. The organic layer was washed with brine, dried with $MgSO_4$, filtered and concentrated under reduced pressure. Purification of the residue by column chromatography (Et_2O/pentane) afforded the title compound **9** (0.88 g, 5.3 mmol, 67%). R_f (10% Et_2O in pentane) = 0.5. ^{1}H NMR (400 MHz, $CDCl_3$) δ 5.51 (d, 6.0 Hz, 1H), 5.04 (d, J = 6.2 Hz, 1H), 4.01 (s, 2H), 3.32 (s, 6H), 1.85 (s, 3H). ^{13}C NMR (101 MHz, $CDCl_3$) δ 137.4, 126.6, 99.6, 52.2, 50.6, 14.9.

(E)-4,4-Dimethoxy-2-methylbut-2-enal (2):

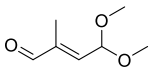

To a stirred solution of **9** (0.78 g. 4.7 mmol) in DMSO (25 mL) was added K_2HPO_4 (1.1 g, 6.2 mmol), KH_2PO_4 (0.23 g, 1.7 mmol) and NaBr (73 mg, 0.71 mmol). The mixture was stirred for 18 hours at 80 °C. Then H_2O was added and the mixture extracted with $CHCl_3$. The organic layer was washed with brine, dried with $MgSO_4$, filtered and concentrated under reduced pressure. Purification of the residue by column chromatography (Et_2O/pentane) afforded the title compound **2** (0.39 g, 2.7 mmol, 57%). R_f (10% Et2O in pentane) = 0.3. ^{1}H NMR (400 MHz, $CDCl_3$) δ 9.49 (s, 1H), 6.39 (d, J = 5.9 Hz, 1H), 5.27 (d, J = 5.9 Hz, 1H), 3.38 (s, 6H), 1.85 (s, 3H); ^{13}C NMR (101 MHz, $CDCl_3$) δ 194.4, 146.7, 141.5, 99.1, 52.5, 9.5. Spectroscopic data are in agreement with those reported.[20]

2-((1E,3E,5E,7E)-9,9-Dimethoxy-3,7-dimethylnona-1,3,5,7-tetraen-1-yl)-1,3,3-trimethyl-5-(prop-2-yn-1-yloxy)cyclohex-1-ene (STA-211):

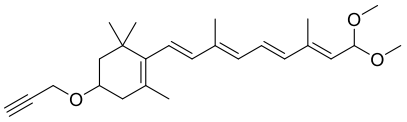

To a stirred solution of **1** (420 mg, 0.70 mmol) in dry THF (5 mL) at -78 °C under N_2 was added *n*-BuLi (0.3 mL, 2.5 M in hexane, 0.76 mmol). The mixture was stirred for 30 minutes at -78 °C and then a solution of **2** (100 mg, 0.70 mmol) in dry THF (5 mL) was added. The reaction mixture was stirred for 1 hour at -78 °C and then for 3 hours at room temperature. The reaction was quenched with sat. aq. NH_4Cl and extracted with Et_2O. The combined organic layers were washed with H_2O and brine, dried with $MgSO_4$, filtered and concentrated under reduced pressure. Purification of the residue by column chromatography (Et_2O/pentane) with neutral silica afforded the title compound **STA-211** (21 mg, 55 µmol, 7.9%). ^{1}H NMR (500 MHz, $CDCl_3$) δ 6.70 – 6.07 (m, 5H), 5.56 – 5.13 (m, 2H), 4.22 (d, *J* = 2.4 Hz, 2H), 3.86 (dtt, *J* = 12.0, 5.7, 3.3 Hz, 1H), 3.33 (d, *J* = 10.1 Hz, 6H), 2.46 – 2.38 (m, 2H), 2.07 (dd, *J* = 16.8, 9.6 Hz, 1H), 1.96 (s, 3H), 1.91 (s, 3H), 1.86 – 1.82 (m, 1H), 1.73 (s, 3H), 1.44 (t, *J* = 12.0 Hz, 1H), 1.07 (s, 6H). ^{13}C NMR (126 MHz, $CDCl_3$) δ 154.6, 138.9, 138.3, 137.7, 136.3, 136.1, 130.4, 127.8, 126.1, 125.9, 125.7, 100.2, 80.4, 73.8, 71.6, 55.1, 52.2, 44.5, 39.2, 36.8, 30.2, 28.6, 21.6, 13.2, 12.7. HRMS (ESI) m/z: $[M + H]^+$ calculated for deprotected **STA-211** $C_{23}H_{30}O_2$: 339.23186, found: 339.23185.

Ethyl (2E,4E/Z,6E,8E)-3,7-dimethyl-9-(2,6,6-trimethyl-4-(prop-2-yn-1-yloxy)cyclohex-1-en-1-yl)nona-2,4,6,8-tetraenoate (4):

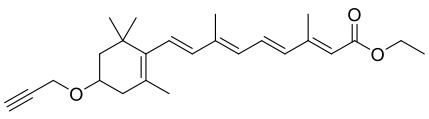

To a stirred solution of **1** (0.50 g, 0.83 mmol) in dry THF (4 mL) at -78 °C under N_2 was added *n*-BuLi (0.50 mL, 1.6 M in hexane, 0.83 mmol). The mixture was stirred for 30 minutes at -78 °C and then ethyl 3-methyl-4-oxocrotonate **3** (0.10 mL, 0.76 mmol) was added. The reaction was stirred for 1 hour at -78 °C and then for 2 hours at room temperature. The reaction was quenched with sat. aq. NH_4Cl and extracted with Et_2O. The combined organic layers were washed with H_2O and brine, dried with $MgSO_4$ and concentrated under reduced pressure. Purification of the residue by column chromatography (EtOAC/pentane) afforded the title compound **4** (0.11 g, 0.30 mmol, 39%) as a yellow oil as an E/Z mixture (1:0.3). R_f (10% EtOAc in pentane) = 0.95. NMR spectra are obtained from the mixture of stereoisomers. ^{1}H NMR (400 MHz, $CDCl_3$) δ 6.98 (dd, *J* = 15.1, 11.4 Hz, 1H), 6.55 – 6.09 (m, 4H), 5.93 – 5.76 (m, 1H), 4.25 – 4.21 (m, 2H), 4.21 – 4.13 (m, 2H), 3.92 – 3.81 (m, 1H), 2.48 – 2.38 (m, 2H), 2.37 – 2.32 (m, 3H), 2.12 – 2.03 (m, 1H), 2.01 – 1.94 (m, 3H), 1.88 – 1.82 (m, 1H), 1.73 (s, 3H), 1.45 (t, *J* = 12.0 Hz, 1H), 1.29 (t, *J* = 7.1 Hz, 3H), 1.11 – 1.05 (m, 6H). ^{13}C NMR (101 MHz, $CDCl_3$) ^{13}C NMR (101 MHz, $CDCl_3$) δ 167.13, 152.54, 139.10, 137.98,

137.59, 135.51, 130.70, 129.95, 127.48, 126.60, 118.79, 80.30, 73.88, 71.48, 59.64, 55.13, 44.39, 39.23, 36.80, 30.16, 28.58, 21.62, 14.32, 13.78, 12.87. HRMS (ESI) m/z: $[M + H]^+$ calculated for $C_{25}H_{34}O_3$: 383.25807, found 383. 25801.

(2E,4E/Z,6E,8E)-3,7-Dimethyl-9-(2,6,6-trimethyl-4-(prop-2-yn-1-yloxy)cyclohex-1-en-1-yl)nona-2,4,6,8-tetraenoic acid (STA-215):

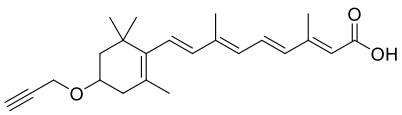

To a stirred solution of **4** (64 mg, 0.167 mmol) in MeOH (2.5 mL) was added 2 M NaOH (aq) (2.5 mL). The reaction was heated at 50 °C for 3 hours and then another 5 mmol of NaOH (200 mg) was added. The reaction was then stirred for 1 hour at 50 °C and then made acidic with 1 M HCl. The product was then extracted with EtOAc, washed with brine, dried over MgSO4, filtered and concentrated. Purification by column chromatography (Et_2O/pentane) afforded the title compound **STA-215** (14 mg, 39 μmol, 24%; 7:3 4E/Z). The E/Z mixture was inseparable and prone to further isomerization under the influence of light. As retinoids are rapidly converted *in vivo* into their biological equilibrium of stereoisomers. **STA-215** was used as the reported E/Z mixture.[30,31] NMR spectra are obtained from the mixture of stereoisomers. ^{1}H NMR (500 MHz, $CDCl_3$) δ 7.04 (dd, *J* = 15.0, 11.4 Hz, 1H), 6.62 – 6.50 (m, 1H), 6.35 – 6.11 (m, 3H), 5.94 – 5.79 (m, 1H), 4.22 (s, 2H), 3.91 – 3.83 (m, 1H), 2.47 – 2.40 (m, 2H), 2.39 – 2.33 (m, 3H), 2.13 – 2.04 (m, 1H), 2.02 – 1.96 (m, 3H), 1.88 – 1.83 (m, 1H), 1.74 (s, 3H), 1.48 – 1.42 (m, 1H), 1.08 (s, 6H). ^{13}C NMR (126 MHz, $CDCl_3$) δ 172.1, 155.1, 139.8, 137.9, 137.6, 135.2, 131.7, 129.9, 127.9, 126.8, 117.8, 80.3, 73.9, 71.5, 55.2, 44.4, 39.2, 36.8, 30.2, 28.6, 21.6, 14.0, 12.9. LC-MS (ESI) m/z: $[M + H]^+$ calculated for $C_{23}H_{30}O_3$: 355.22677, found: 355.16667.

Biological methods

Cell culture. HL60 cells were grown in RPMI with stable glutamine and phenol red with 10% Fetal Calf serum, penicillin and streptomycin at 37 °C and 5% CO_2. Cells were cultured between $0.2*10^6$ and $2.0*10^6$ cells/mL confluence. A549 cells were grown in DMEM with stable glutamine and phenol red with 10% New Born Calf serum, penicillin and streptomycin at 37 °C and 5% CO_2. Medium was refreshed every 2-3 days and cells were passaged twice a week. Cell lines were purchased from ATCC and were regularly tested for mycoplasma contamination. Cultures were discarded after 2-3 months of use.

HL60 differentiation and FACS protocol. HL60 cells were cultured as described above. $2.4*10^6$ cells per condition were collected in a 15 mL tube, the growth medium was removed and replaced with 6 mL medium containing DMSO (1.25% v/v), **STA-215** (1 μM), RA (1 μM) or a combination hereof. Cells were divided over 3 wells in a 6-wells plate and cultured for 72 hours. Cells were counted using a TC20™ automated cell counter and a maximum of $1.0x10^6$ cells was transferred to an Eppendorf tube and centrifuged (500 *g*, 3 min). Cells were suspended in FACS buffer (100 μL; 1% FCS, 1% BSA, 0.1% NaN_3 and 2 mM EDTA in PBS) containing human FcR blocking reagent (4 μL; Miltenyi Biotec), transferred to a V-bottom 96-wells plate and split providing the isotype control samples. Cells were incubated for 10 minutes in the dark at 4 °C. Then staining mixture (50 μL; FACS buffer (4.65 μL), antibody (1 μL) and 7-AAD (2 μg/mL)) was added containing either the CD11b-APC antibody (Miltenyi Biotec) or rat IgG2b-APC (Miltenyi Biotec). Samples were mixed and incubated for 30 minutes in the dark at 4 °C. PBS (200 μL) was added and the plate was centrifuged (500 *g*, 3 min). Cells were suspended in PBS (100 μL) and fixated by adding 1% PFA in PBS (100 μL). After incubating for 15 minutes in the dark at 4 °C PBS was added (200 μL) and the plate was centrifuged. This was repeated once and cells were suspended in FACS buffer (200 μL). Samples were diluted 10x in a new plate to ensure a cell density of <1000 cells/μL. Samples were measured on a Guava® easyCyte™ system. Samples were gated on living single cells and the isotype control was used to gate for background signal for differentiation. Using these settings the percentage of differentiated cells was determined.

Human dendritic cell culture. Peripheral blood mononuclear cells (PBMCs) were isolated by gradient centrifugation of peripheral blood obtained from healthy donors on lymphoprep (d=1.077, Fresenius Kabi, Bad Homburg, Germany). Blood was drawn after receiving signed informed consent according to the guidelines of the Medical Ethical Committee of the VU University Medical Center (Amsterdam, the Netherlands) in accordance with the Declaration of Helsinki. $CD14^+$ monocytes were isolated from the PBMC fraction with positive selection using CD14 magnetic microbeads (Miltenyi Biotec, Leiden, the Netherlands). $CD14^+$ cells were cultured in RPMI supplemented with 10% FCS, 1%PSG, 20 ng/ml GM-CSF and 20 ng/ml IL-4 (both Immunotools, Friesoythe, Germany) for 6 days in order to induce the development of dendritic cells in the presence of 10 μM retinoic acid, retinal, (both Sigma Aldrich, Zwijndrecht, the Netherlands) **STA-211**, **STA-215** or a vehicle control.

At day 6, cells were harvested and an ALDEFLUOR assay (Stemcell, Cologne, Germany) was performed according to manufacturer's protocol. Cells were subsequently stained with CD1c BV421 (1:20, clone L161, Biolegend, London, United Kingdom), CD14 BV510 (1:25, clone MφP9, BD Bioscience, San Jose, CA, USA), CD86 PE (1:100, clone 2331, BD Bioscience, San Jose, CA, USA) and CD103 APC (1:20, clone Ber-ACT8, BD Bioscience, San Jose, CA, USA). Before acquisition 7-AAD was added as a live death marker. Samples were acquired on LSR-Fortessa X20 (BD Bioscience, Mountain View, CA, USA) and data was analyzed with Flowjo software (Tree Star, San Carlos, CA, USA).

***In situ* affinity-based protein profiling. STA-211** was deprotected by dilution in MilliQ or acidic buffer. Growth medium from cells grown in 6-wells plate was removed and 1 mL serum free medium containing probe **STA-211** (10 µM, 0.1% EtOH) or **STA-215** (10 µM, 0.1% EtOH) was added. The cells were incubated for 1 hour. For competitive A*f*BPP cells were first incubated with vehicle or competitor (100 µM, 0.1% EtOH) for 30 minutes followed by **STA-211** (10 µM final concentration) or **STA-215** (10 µM final concentration) for 1 hour. The medium was then removed, the cells were washed with 2 mL PBS and then irradiated (350 nm, 10 min) in 1 mL ice-cold PBS. The cells were then harvested using a cell scraper and transferred to an Eppendorf tube and the suspension was centrifuged for 5 minutes at 1200 rpm. The PBS was removed and the samples snap frozen and stored at -80 °C until further use.

Copper-catalysed azide-alkyne cycloaddition reaction and in-gel fluorescence analysis. Cell pellets were thawed on ice, lysed by addition of ice-cold lysis buffer (MilliQ, 1x protease inhibitor cocktail (Roche c*O*mplete EDTA free)) and incubated on ice (15-30 min). The protein concentration was determined by a Quick Start™ Bradford Protein assay (Bio-Rad). The protein fractions were diluted to a total protein concentration of 1 mg/mL. From each sample 40 µL was taken and treated with 5 µL from a freshly prepared "click" mixture containing 9 mM $CuSO_4$ (2.5 µL/sample, 18 mM in H_2O), 45 mM NaAsc (1.5 µL/sample, 150 mM in H_2O), 1.8 mM THPTA (0.5 µL/sample, 18 mM in DMSO) and 9 µM Alexa Fluor 647 azide (0.5 µL/sample, 90 µM in DMSO from Thermo Fischer Scientific). The samples were incubated for 1 hour at 37 °C and then 15 µL 4x SDS page sample buffer was added. The samples were denatured at 100 °C for 5 minutes. 8 µg per sample was resolved on a SDS-PAGE gel (10% acrylamide, 180V, 75 min). Gels were visualized with a ChemiDoc XRS (Bio-Rad) using Cy3 and Cy5 multichannel settings (605/50 and 695/55, filters respectively) and stained with Coomassie. Fluorescence was normalized to Coomassie staining.

Imaging flow cytometry. A549 cells were incubated with **STA-211** (10 µM), **STA-215** (10 µM) or a vehicle control (ethanol) for 1 hour under serum-free conditions. Cells were then fixated using 1% PFA. Click chemistry mixture (click mix) was prepared (1 mM CuSO4, 5 mM NaAsc, 0.4 mM THPTA (all Sigma Aldrich, Zwijndrecht, the Netherlands), 40 µM biotin-alkyne, Alexa Fluor 488-azide (all Click Chemistry Tools, Scottsdale, AZ, United States) and PBS was added. Samples were incubated for 1 hour at 37 °C. DAPI was added as a nuclear stain just before acquisition. Samples were analyzed using the ImageStream. The ImageStream is an instrument that combines flow cytometry and microscopy in one platform and is thereby able to generate population statistics on subcellular morphological measurements made per cell across a sample of thousands. The system has a magnification lens in the light path after the flow cell and in essence replaces the PMT's of a conventional flow cytometer with a camera. It is thus able to image thousands of cells per second with microscopic resolution. Sample were acquired using the INSPIRE acquisition software on a two camera, 4 laser (125mW 405nm, 100mW 488 nm, 200 mW 561 nm, 150mW 642 nm) ImageStream ISX from Amnis (a Luminex subsidiary). With the 488nm laser and 405nm laser set at 100 mW and 125 mW respectively, the Alexa Fluor 488 signal was measured in Channel 2 of Camera 1 and the DAPI signal was measured in Channel 7 of Camera 2. The magnification was set at 60x with a sample core velocity of 40mm/min. The acquired images and data were analyzed using the image analysis software IDEAS. IDEAS is flexible and powerful enough to identify and measure any discernible object in an image. To this end, a threshold mask of 70% of the default DAPI mask was created for the nucleus and the extent of nuclear translocation for the clickable vitamins was quantified using this nuclear mask as the region of interest for both the Bright Detail Similarity and Internalization features in the IDEAS software.

In situ activity-based proteomics

Sample preparation. Protocol adapted from previously described procedure.[32] Cells were treated *in situ*, irradiated, harvested, lysed and adjusted to 1 mg/mL protein concentration as described above. 250 µL was taken from each sample and to this 25 µL freshly prepared "click" mixture containing 1 mM $CuSO_4$ (2.5 µL/sample, 100 mM in H_2O), 5 mM NaAsc (1.25 µL/sample, 1M in H_2O), 0.4 mM THPTA (1 µL/sample, 100 mM in DMSO), 40 µM biotin-alkyne (2.5 µL/sample, 4 mM in DMSO) and MilliQ (17.75 µL/sample) was added. Samples were incubated for 1 hour at 37 °C while shaking (300 rpm). Excess click reagents were then removed by chloroform/methanol precipitation followed by another wash with methanol. Precipitated proteomes were then suspended in urea buffer (250 µL, 6 M urea and 25 mM ammonium bicarbonate), DTT (2.5 µL, 1M) was added and the mixture was then incubated for 15 min at 65 °C while shaking (600 rpm). The samples were then allowed to cool down to RT and then alkylated by addition of iodoacetamide (20 µL, 0.5M) for 30 minutes at RT in the dark. Addition of SDS (70 µL, 10% (v/v)) was followed by heating at 65 °C for 5 minutes. For each sample 50 µL 50% slurry of avidin-agarose beads from egg white (Sigma-Aldrich) was washed three times with PBS and transferred in PBS (1 mL) to a 15 mL tube. To this another 2 mL of PBS was added followed by the corresponding proteome sample. The beads were incubated with the proteome for 2 hours at room temperature using an overhead shaker. The beads were then isolated by centrifugation (2 min, 2500 g), washed with SDS in PBS (0.5% (w/v)) and washed three times with PBS. The beads were then transferred to low-binding Eppendorf tubes and proteins were digested overnight at 37 °C and 950 rpm shaking in 250 µL digestion buffer (100 mM Tris, 100 mM NaCl, 1 mM $CaCl_2$, 2% acetonitrile and 0.5 µg sequencing grade trypsin (Promega)). Digestion was stopped by addition of formic acid (12.5 µL) and the beads were filtered off by centrifugation (2 min, 600 g) using a Bio-Spin column (Bio-Rad). Samples were then desalted using stage tips, collected in low-binding Eppendorf tubes, concentrated using a SpeedVac (Eppendorf) and stored at -20 °C until reconstitution before measurement.[33] All samples were prepared in at least three biological replicates.

LC-MS/MS measurement and analysis. Samples were reconstituted in LC-MS sample solution (50 µL, MilliQ, 3% acetonitrile/0.1% formic acid/20 fmol/µL enolase). Samples were then analysed using a NanoACQUITY UPLC System (Waters) coupled to a SYNAPT G2-Si high-definition mass spectrometer (Waters) as previously described.[32,34] Of each sample 5 µL was loaded on a nanoEASE™ M/Z Symmetry C18 trap column (particles 5 µm, 100 Å , 180 µm x 20 mm, Waters) with 0.1% formic acid and separated on an nanoEASE™ M/Z HSS C18 T3 analytical column (particles 1.8 µm, 75 µm x 250 mm, Waters) heated at 80 °C. A multistep gradient running from 5-40% acetonitrile containing 0.1% formic acid during a 70 minute method at 300 nL/min was used to achieve peptide separation. Survey scans (m/z 50-2000 Da) were acquired in the Synapt with a scan time of 0.6 seconds in positive, resolution mode. The collision energy is set to 4 V in the trap cell for low-energy MS mode. For the elevated energy scan, the transfer cell collision energy is ramped using drift-time specific collision energies. The lock mass is sampled every 30 seconds. MS raw files were analysed with ProteinLynx Global SERVER (PLGS, v3.0.3, Waters). The MS^E identification was also performed with PLGS using the human proteome from Uniprot (Uniprot-homo-sapiens-trypsin-reviewed-2016-08-29.fasta). The following parameter settings were used: low energy threshold 150 counts, elevated energy threshold 30, peptide and protein FDR 1%, enzyme specificity trypsin, max missed cleavages max 2, variable modification methionine oxidation, fixed modification carbamidomethylation cysteine, at least fragments/peptide 2, fragments/protein 5, peptides/protein 1 and number of peptides to measure per protein 3. For label-free quantification ISOQuant (v1.5) was used.[35,36] Data were filtered to retain only proteins with two or more reported unique peptides and quantified in at least 3 replicates of the positive control (probe-treated). Proteins were designated as significantly enriched by the probe when they showed 2-fold enrichment in quantification value when comparing negative control (vehicle-treated) with positive control (probe-treated) samples and probability as determined by a Student's *t* test (<0.05).

Supplementary Data

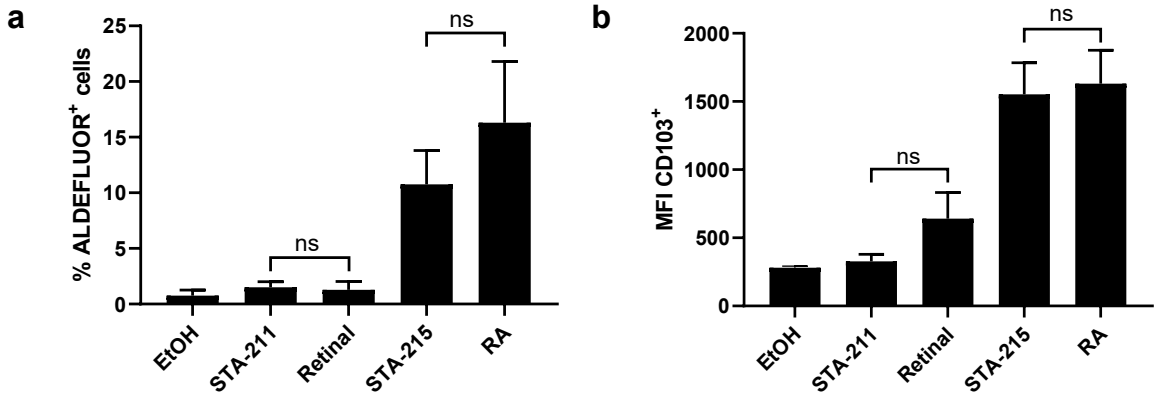

Supplementary Fig. 7.1 | Clickable retinoid (10 µM) induced differentiation of dendritic cells. a, Graph showing the general ALDH activity of activated dendritic cells as determined by the ALDEFLUOR assay. **b**, Graph showing the differentiation of dendritic cells as measured by the expression of the CD103 marker. For parts **a** and **b**, data represent mean values ± SD. *N* = 3 experiments per group (biological replicates).

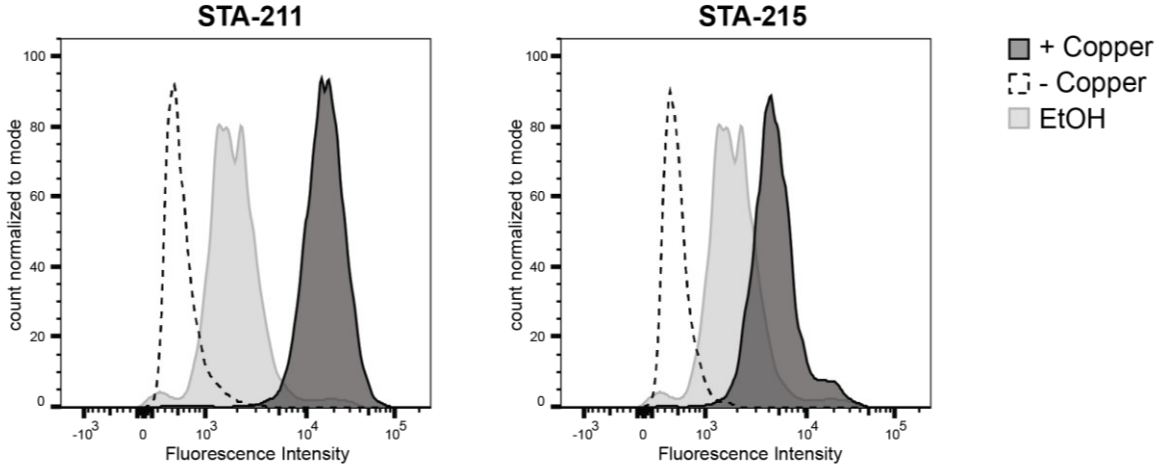

Supplementary Fig. 7.2 | Flow cytometry approach to visualize clickable vitamins in A549 cells. Fluorescence intensity of Alexa Fluor 488 conjugated to clickable vitamins of cells treated with vehicle (EtOH), **STA-211** (10 µM) or **STA-215** (10 µM).

Supplementary Table 7.1 | Proteins significantly enriched by STA-215 (10 µM) in HL60 cells corresponding to Fig. 7.3b,c.

Name	Accession	Uniprot ID	Fold-change (UV/noUV)	Significance ($-\log_{10}$)	RA competed
Phosphoglycerate kinase 2	P07205	PGK2_HUMAN	20.0	7.7	Yes
Endoplasmic reticulum junction formation protein lunapark	Q9C0E8	LNP_HUMAN	20.0	4.9	Yes
Peroxiredoxin-4	Q13162	PRDX4_HUMAN	20.0	4.8	Yes
Dynamin-like 120 kDa protein_ mitochondrial	O60313	OPA1_HUMAN	20.0	4.5	Yes
ATPase family AAA domain-containing protein 1	Q8NBU5	ATAD1_HUMAN	20.0	4.4	Yes
Tubulin beta-6 chain	Q9BUF5	TBB6_HUMAN	20.0	4.2	Yes
Protein SCO2 homolog_ mitochondrial	O43819	SCO2_HUMAN	20.0	3.6	Yes
Membrane-associated progesterone receptor component 2	O15173	PGRC2_HUMAN	2.0	2.3	Yes
Retinol dehydrogenase 11	Q8TC12	RDH11_HUMAN	20.0	1.6	Yes
Fatty aldehyde dehydrogenase	P51648	AL3A2_HUMAN	20.0	1.5	Yes
Ubiquitin-associated domain-containing protein 2	Q8NBM4	UBAC2_HUMAN	20.0	1.5	Yes
Nucleoside diphosphate kinase B	P22392	NDKB_HUMAN	20.0	5.7	Yes
Keratin_ type I cytoskeletal 19	P08727	K1C19_HUMAN	2.9	1.5	No
Alpha-2-HS-glycoprotein	P02765	FETUA_HUMAN	2.3	2.2	No
Golgi phosphoprotein 3	Q9H4A6	GOLP3_HUMAN	20.0	4.4	Yes
Neutral cholesterol ester hydrolase 1	Q6PIU2	NCEH1_HUMAN	20.0	4.9	Yes
Transmembrane emp24 domain-containing protein 10	P49755	TMEDA_HUMAN	8.3	3.9	Yes
ATPase ASNA1	O43681	ASNA_HUMAN	20.0	4.5	Yes
Translocation protein SEC63 homolog	Q9UGP8	SEC63_HUMAN	2.3	2.6	Yes
Transmembrane protein 214	Q6NUQ4	TM214_HUMAN	3.0	3.6	Yes
Protein FAM162A	Q96A26	F162A_HUMAN	20.0	2.4	Yes
Sarcoplasmic/endoplasmic reticulum calcium ATPase 3	Q93084	AT2A3_HUMAN	3.7	3.3	Yes
ADP-ribosylation factor 4	P18085	ARF4_HUMAN	3.0	2.2	No
Transmembrane protein 43	Q9BTV4	TMM43_HUMAN	3.4	3.5	Yes
Very-long-chain 3-oxoacyl-CoA reductase	Q53GQ0	DHB12_HUMAN	6.4	3.5	Yes
Alkyldihydroxyacetonephosphate synthase_ peroxisomal	O00116	ADAS_HUMAN	2.3	3.6	Yes
Thioredoxin-related transmembrane protein 1	Q9H3N1	TMX1_HUMAN	3.3	4.1	Yes
Transmembrane protein 109	Q9BVC6	TM109_HUMAN	4.6	5.1	Yes
Adipocyte plasma membrane-associated protein	Q9HDC9	APMAP_HUMAN	2.7	3.3	Yes
Ras-related protein Rab-14	P61106	RAB14_HUMAN	20.0	3.4	Yes
Monocarboxylate transporter 1	P53985	MOT1_HUMAN	2.4	3.6	Yes
Erlin-1	O75477	ERLN1_HUMAN	20.0	8.0	Yes
Translocation protein SEC62	Q99442	SEC62_HUMAN	2.6	4.0	Yes
BRI3-binding protein	Q8WY22	BRI3B_HUMAN	3.4	4.0	Yes
Vesicular integral-membrane protein VIP36	Q12907	LMAN2_HUMAN	3.9	4.7	Yes
Lysosome-associated membrane glycoprotein 1	P11279	LAMP1_HUMAN	20.0	1.6	No
Very-long-chain enoyl-CoA reductase	Q9NZ01	TECR_HUMAN	2.1	2.9	Yes
Long-chain-fatty-acid--CoA ligase 1	P33121	ACSL1_HUMAN	20.0	4.5	Yes
Cation-dependent mannose-6-phosphate receptor	P20645	MPRD_HUMAN	3.6	3.3	Yes
Transmembrane emp24 domain-containing protein 9	Q9BVK6	TMED9_HUMAN	3.0	3.3	Yes
Down syndrome cell adhesion molecule-like protein 1	Q8TD84	DSCL1_HUMAN	2.2	2.1	No
Very-long-chain (3R)-3-hydroxyacyl-CoA dehydratase 3	Q9P035	HACD3_HUMAN	2.7	3.3	No
Cytochrome b-c1 complex subunit 7	P14927	QCR7_HUMAN	20.0	3.6	No
Derlin-1	Q9BUN8	DERL1_HUMAN	20.0	7.6	No
Major facilitator superfamily domain-containing protein 10	Q14728	MFS10_HUMAN	2.4	2.5	No
Nuclear pore membrane glycoprotein 210	Q8TEM1	PO210_HUMAN	2.1	1.5	No
Dolichyl-diphosphooligosaccharide--protein glycosyltransferase 48 kDa subunit	P39656	OST48_HUMAN	2.3	4.0	No
Endoplasmic reticulum resident protein 29	P30040	ERP29_HUMAN	3.3	4.2	No
Voltage-dependent anion-selective channel protein 1	P21796	VDAC1_HUMAN	12.2	4.4	No
Probable ergosterol biosynthetic protein 28	Q9UKR5	ERG28_HUMAN	3.1	4.4	No
Reticulon-4	Q9NQC3	RTN4_HUMAN	2.9	1.4	No
Endoplasmic reticulum chaperone BiP	P11021	BIP_HUMAN	2.2	3.5	No
Dolichyl-diphosphooligosaccharide--protein glycosyltransferase subunit 2	P04844	RPN2_HUMAN	2.5	4.3	No
Signal recognition particle receptor subunit beta	Q9Y5M8	SRPRB_HUMAN	3.6	4.3	No
Lanosterol synthase	P48449	ERG7_HUMAN	2.2	3.4	No
3-beta-hydroxysteroid-Delta(8)_Delta(7)-isomerase	Q15125	EBP_HUMAN	3.1	2.5	No
Receptor expression-enhancing protein 4	Q9H6H4	REEP4_HUMAN	3.9	4.5	No
Dolichyl-diphosphooligosaccharide--protein glycosyltransferase subunit STT3B	Q8TCJ2	STT3B_HUMAN	2.4	3.4	No
Receptor expression-enhancing protein 5	Q00765	REEP5_HUMAN	2.1	1.9	No
Apolipoprotein A-I	P02647	APOA1_HUMAN	18.9	1.8	No
Monocarboxylate transporter 4	O15427	MOT4_HUMAN	2.9	2.8	No
Cullin-associated NEDD8-dissociated protein 1	Q86VP6	CAND1_HUMAN	3.7	2.6	No
Extended synaptotagmin-1	Q9BSJ8	ESYT1_HUMAN	10.9	4.0	No
Cleft lip and palate transmembrane protein 1-like protein	Q96KA5	CLP1L_HUMAN	3.8	3.1	No
AFG3-like protein 2	Q9Y4W6	AFG32_HUMAN	20.0	5.6	No
Sigma intracellular receptor 2	Q5BJF2	SGMR2_HUMAN	20.0	3.0	No
Transmembrane protein 33	P57088	TMM33_HUMAN	2.6	3.8	No
Carnitine O-palmitoyltransferase 1_ liver isoform	P50416	CPT1A_HUMAN	3.6	3.6	No
NADH-cytochrome b5 reductase 3	P00387	NB5R3_HUMAN	2.1	1.7	No
Dolichyl-diphosphooligosaccharide--protein glycosyltransferase subunit 1	P04843	RPN1_HUMAN	2.2	3.6	No
Large neutral amino acids transporter small subunit 1	Q01650	LAT1_HUMAN	2.8	3.2	No
Voltage-dependent anion-selective channel protein 2	P45880	VDAC2_HUMAN	8.8	4.5	No
B-cell receptor-associated protein 31	P51572	BAP31_HUMAN	3.0	1.7	No
Keratin_ type II cytoskeletal 1b	Q7Z794	K2C1B_HUMAN	20.0	3.2	No
CAAX prenyl protease 1 homolog	O75844	FACE1_HUMAN	2.5	2.6	No
Protein kish-A	Q8TBQ9	KISHA_HUMAN	2.4	3.0	No
Protein transport protein Sec61 subunit alpha isoform 1	P61619	S61A1_HUMAN	2.8	3.4	No
Atlastin-3	Q6DD88	ATLA3_HUMAN	20.0	4.1	No
Protein disulfide-isomerase TMX3	Q96JJ7	TMX3_HUMAN	2.0	3.2	No
Basigin	P35613	BASI_HUMAN	2.8	3.5	No
Protein disulfide-isomerase	P07237	PDIA1_HUMAN	2.7	4.7	No
Translocon-associated protein subunit alpha	P43307	SSRA_HUMAN	3.2	3.7	No
Inactive hydroxysteroid dehydrogenase-like protein 1	Q3SXM5	HSDL1_HUMAN	20.0	4.4	No
Lysophosphatidylcholine acyltransferase 2	Q7L5N7	PCAT2_HUMAN	2.3	4.0	No
Protein YIPF5	Q969M3	YIPF5_HUMAN	2.1	1.8	No
ADP-ribosylation factor-like protein 6-interacting protein 1	Q15041	AR6P1_HUMAN	20.0	2.9	No
Acylglycerol kinase_ mitochondrial	Q53H12	AGK_HUMAN	20.0	4.8	No
Mitochondrial fission process protein 1	Q9UDX5	MTFP1_HUMAN	20.0	3.4	No

Name	Accession	Uniprot ID	Fold-change (UV/noUV)	Significance ($-\log_{10}$)	RA competed
Heat shock protein beta-1	P04792	HSPB1_HUMAN	2.1	2.8	No
Reticulon-3	O95197	RTN3_HUMAN	2.8	2.6	No
Translocator protein	P30536	TSPO_HUMAN	3.3	3.6	No
Translocon-associated protein subunit delta	P51571	SSRD_HUMAN	3.9	3.7	No
4F2 cell-surface antigen heavy chain	P08195	4F2_HUMAN	20.0	4.7	No
Leukocyte surface antigen CD47	Q08722	CD47_HUMAN	2.1	2.8	No
Voltage-dependent anion-selective channel protein 3	Q9Y277	VDAC3_HUMAN	6.7	4.0	No
Prohibitin-2	Q99623	PHB2_HUMAN	7.0	5.1	No
Calcium-binding mitochondrial carrier protein Aralar1	O75746	CMC1_HUMAN	20.0	4.6	No
Serum albumin	P02768	ALBU_HUMAN	3.7	3.1	No
Calcium-binding mitochondrial carrier protein Aralar2	Q9UJS0	CMC2_HUMAN	20.0	6.2	No
Keratin_ type II cytoskeletal 6B	P04259	K2C6B_HUMAN	20.0	2.6	No
Prohibitin	P35232	PHB_HUMAN	4.8	6.3	No
Sarcoplasmic/endoplasmic reticulum calcium ATPase 2	P16615	AT2A2_HUMAN	2.1	3.9	No
NADH dehydrogenase [ubiquinone] 1 alpha subcomplex subunit 10_ mitochondrial	O95299	NDUAA_HUMAN	20.0	4.2	No
Ras-related protein Rab-10	P61026	RAB10_HUMAN	2.7	3.4	No
Neutral amino acid transporter B(0)	Q15758	AAAT_HUMAN	3.2	4.5	No
Myeloid-associated differentiation marker	Q96S97	MYADM_HUMAN	3.2	3.7	No
Ras-related protein Rab-39A	Q14964	RB39A_HUMAN	20.0	4.6	No
Dolichyl-diphosphooligosaccharide--protein glycosyltransferase subunit DAD1	P61803	DAD1_HUMAN	2.3	2.7	No
Sodium/potassium-transporting ATPase subunit beta-3	P54709	AT1B3_HUMAN	4.0	4.3	No
Ras-related C3 botulinum toxin substrate 2	P15153	RAC2_HUMAN	2.0	2.8	No
Mitochondrial import inner membrane translocase subunit TIM50	Q3ZCQ8	TIM50_HUMAN	5.2	5.8	No
Calcium load-activated calcium channel	Q9UM00	TMCO1_HUMAN	2.4	3.9	No
Sodium/potassium-transporting ATPase subunit alpha-2	P50993	AT1A2_HUMAN	11.8	1.9	No
NADH dehydrogenase [ubiquinone] 1 beta subcomplex subunit 8_ mitochondrial	O95169	NDUB8_HUMAN	20.0	3.7	No
Arachidonate 5-lipoxygenase-activating protein	P20292	AL5AP_HUMAN	2.2	1.7	No
Ras-related protein Rap-1b	P61224	RAP1B_HUMAN	2.1	2.6	No
Ubiquitin-60S ribosomal protein L40	P62987	RL40_HUMAN	2.6	5.0	No
Mitochondrial import receptor subunit TOM40 homolog	O96008	TOM40_HUMAN	3.0	3.5	No
ADP-dependent glucokinase	Q9BRR6	ADPGK_HUMAN	20.0	2.8	No
Sorting and assembly machinery component 50 homolog	Q9Y512	SAM50_HUMAN	20.0	6.4	No
Dol-P-Man:Man(5)GlcNAc(2)-PP-Dol alpha-1_3-mannosyltransferase	Q92685	ALG3_HUMAN	2.6	1.8	No
ATPase family AAA domain-containing protein 3A	Q9NVI7	ATD3A_HUMAN	2.3	3.7	No
GDP-Man:Man(3)GlcNAc(2)-PP-Dol alpha-1_2-mannosyltransferase	Q2TAA5	ALG11_HUMAN	2.9	3.9	No
Protein disulfide-isomerase A6	Q15084	PDIA6_HUMAN	2.3	2.7	No
Sigma non-opioid intracellular receptor 1	Q99720	SGMR1_HUMAN	6.6	4.2	No
ATPase family AAA domain-containing protein 3B	Q5T9A4	ATD3B_HUMAN	2.0	4.0	No
GPI-anchor transamidase	Q92643	GPI8_HUMAN	20.0	5.1	No
Estradiol 17-beta-dehydrogenase 11	Q8NBQ5	DHB11_HUMAN	2.4	2.8	No
CDGSH iron-sulfur domain-containing protein 2	Q8N5K1	CISD2_HUMAN	20.0	1.4	No
Phosphatidate cytidylyltransferase_ mitochondrial	Q96BW9	TAM41_HUMAN	20.0	3.6	No
Protein disulfide-isomerase A3	P30101	PDIA3_HUMAN	2.3	4.1	No
Equilibrative nucleoside transporter 1	Q99808	S29A1_HUMAN	3.0	3.4	No
NADH dehydrogenase [ubiquinone] 1 beta subcomplex subunit 11_ mitochondrial	Q9NX14	NDUBB_HUMAN	20.0	4.2	No
Myosin-11	P35749	MYH11_HUMAN	2.5	2.6	No
MICOS complex subunit MIC60	Q16891	MIC60_HUMAN	3.4	4.6	No
Lysocardiolipin acyltransferase 1	Q6UWP7	LCLT1_HUMAN	2.9	2.8	No
Cytochrome c-type heme lyase	P53701	CCHL_HUMAN	20.0	3.8	No
Sideroflexin-1	Q9H9B4	SFXN1_HUMAN	2.9	4.3	No
Mitochondrial inner membrane protein OXA1L	Q15070	OXA1L_HUMAN	4.6	4.4	No
Guanine nucleotide-binding protein G(o) subunit alpha	P09471	GNAO_HUMAN	2.4	2.5	No
Signal peptidase complex subunit 3	P61009	SPCS3_HUMAN	20.0	1.5	No
DnaJ homolog subfamily C member 11	Q9NVH1	DJC11_HUMAN	20.0	5.8	No
Tricarboxylate transport protein_ mitochondrial	P53007	TXTP_HUMAN	2.2	4.8	No
ADP/ATP translocase 3	P12236	ADT3_HUMAN	3.3	3.8	No
Microsomal glutathione S-transferase 3	O14880	MGST3_HUMAN	3.2	2.6	No
GTP-binding protein SAR1a	Q9NR31	SAR1A_HUMAN	2.2	1.7	No
Tetratricopeptide repeat protein 39C	Q8N584	TT39C_HUMAN	20.0	5.0	No
Lamina-associated polypeptide 2_ isoforms beta/gamma	P42167	LAP2B_HUMAN	2.1	2.5	No
Phosphate carrier protein_ mitochondrial	Q00325	MPCP_HUMAN	4.4	5.2	No
Ras-related protein Rab-8A	P61006	RAB8A_HUMAN	2.1	1.8	No
Mitochondrial import receptor subunit TOM70	O94826	TOM70_HUMAN	20.0	6.4	No
Apolipoprotein M	O95445	APOM_HUMAN	20.0	3.2	No
Cytochrome c oxidase subunit 2	P00403	COX2_HUMAN	2.2	2.7	No
Squalene synthase	P37268	FDFT_HUMAN	2.3	3.0	No
Ras-related protein Rab-5C	P51148	RAB5C_HUMAN	20.0	4.2	No
Vitamin K epoxide reductase complex subunit 1-like protein 1	Q8N0U8	VKORL_HUMAN	20.0	3.5	No
ADP/ATP translocase 2	P05141	ADT2_HUMAN	9.8	6.2	No
Mitochondrial dicarboxylate carrier	Q9UBX3	DIC_HUMAN	20.0	6.0	No
ATP synthase subunit g_ mitochondrial	O75964	ATP5L_HUMAN	2.9	3.8	No
Thioredoxin domain-containing protein 5	Q8NBS9	TXND5_HUMAN	2.1	3.5	No
ATP-binding cassette sub-family D member 3	P28288	ABCD3_HUMAN	20.0	6.8	No
MICOS complex subunit MIC13	Q5XKP0	MIC13_HUMAN	20.0	2.6	No
Vesicle-associated membrane protein 8	Q9BV40	VAMP8_HUMAN	2.5	2.2	No
Protein ERGIC-53	P49257	LMAN1_HUMAN	3.0	4.4	No
Membrane-associated progesterone receptor component 1	O00264	PGRC1_HUMAN	2.9	2.6	No
Synaptic vesicle membrane protein VAT-1 homolog	Q99536	VAT1_HUMAN	2.7	3.9	No
Solute carrier family 43 member 3	Q8NBI5	S43A3_HUMAN	20.0	3.6	No
Hemoglobin subunit alpha	P69905	HBA_HUMAN	2.7	2.2	No
NADH dehydrogenase [ubiquinone] 1 alpha subcomplex subunit 9_ mitochondrial	Q16795	NDUA9_HUMAN	2.2	2.4	No
Mitochondrial import receptor subunit TOM20 homolog	Q15388	TOM20_HUMAN	2.3	2.0	No
Mitochondrial proton/calcium exchanger protein	O95202	LETM1_HUMAN	2.5	3.1	No
ATP-binding cassette sub-family B member 10_ mitochondrial	Q9NRK6	ABCBA_HUMAN	2.5	3.7	No
Guanine nucleotide-binding protein subunit alpha-13	Q14344	GNA13_HUMAN	3.5	5.9	No
Ran-specific GTPase-activating protein	P43487	RANG_HUMAN	20.0	1.6	No
14-3-3 protein epsilon	P62258	1433E_HUMAN	2.7	1.9	No

Name	Accession	Uniprot ID	Fold-change (UV/noUV)	Significance ($-\log_{10}$)	RA competed
Phosphatidylinositol glycan anchor biosynthesis class U protein	Q9H490	PIGU_HUMAN	2.1	1.9	No
NADH dehydrogenase [ubiquinone] 1 beta subcomplex subunit 4	O95168	NDUB4_HUMAN	20.0	8.4	No
Emerin	P50402	EMD_HUMAN	20.0	5.6	No
Fatty acyl-CoA reductase 1	Q8WVX9	FACR1_HUMAN	20.0	1.6	No
Minor histocompatibility antigen H13	Q8TCT9	HM13_HUMAN	20.0	1.6	No
Calcium-binding mitochondrial carrier protein SCaMC-1	Q6NUK1	SCMC1_HUMAN	20.0	1.6	No
Ras-related protein Rab-27A	P51159	RB27A_HUMAN	20.0	1.6	No
Mitochondrial carrier homolog 2	Q9Y6C9	MTCH2_HUMAN	3.1	2.4	No
ADP-ribosylation factor 1	P84077	ARF1_HUMAN	3.6	3.4	No
Catechol O-methyltransferase	P21964	COMT_HUMAN	20.0	1.5	No
Mitochondrial import inner membrane translocase subunit TIM44	O43615	TIM44_HUMAN	20.0	7.3	No
Peptidyl-tRNA hydrolase 2_ mitochondrial	Q9Y3E5	PTH2_HUMAN	20.0	2.8	No
OCIA domain-containing protein 1	Q9NX40	OCAD1_HUMAN	2.6	3.3	No
Spliceosome RNA helicase DDX39B	Q13838	DX39B_HUMAN	20.0	5.8	No
Cytochrome c oxidase subunit 6C	P09669	COX6C_HUMAN	20.0	1.5	No
Ras-related protein Rab-1A	P62820	RAB1A_HUMAN	2.7	2.7	No
POTE ankyrin domain family member E	Q6S8J3	POTEE_HUMAN	20.0	6.4	No

Supplementary Table 7.2 | Proteins significantly enriched by LEI-945 (1 µM) in HL60 cells.

Name	Accession	Uniprot ID	Fold-change (LEI-945/DMSO)	Significance ($-\log_{10}$)
Voltage-dependent anion-selective channel protein 1	P21796	VDAC1_HUMAN	3.2	5.0
Ubiquitin-60S ribosomal protein L40	P62987	RL40_HUMAN	4.6	4.7
Voltage-dependent anion-selective channel protein 2	P45880	VDAC2_HUMAN	20.0	8.9
ADP/ATP translocase 2	P05141	ADT2_HUMAN	4.7	6.6
L-lactate dehydrogenase B chain	P07195	LDHB_HUMAN	2.0	3.7
Dolichyl-diphosphooligosaccharide--protein glycosyltransferase subunit DAD1	P61803	DAD1_HUMAN	3.2	6.3
Prohibitin-2	Q99623	PHB2_HUMAN	2.3	3.4
Microsomal glutathione S-transferase 3	O14880	MGST3_HUMAN	20.0	4.6
Tubulin alpha-1C chain	Q9BQE3	TBA1C_HUMAN	2.0	4.2
Voltage-dependent anion-selective channel protein 3	Q9Y277	VDAC3_HUMAN	20.0	5.6
ADP/ATP translocase 3	P12236	ADT3_HUMAN	3.2	5.7
Up-regulated during skeletal muscle growth protein 5	Q96IX5	USMG5_HUMAN	3.4	4.5
Protein disulfide-isomerase	P07237	PDIA1_HUMAN	8.1	7.9
Ras-related protein Rab-1A	P62820	RAB1A_HUMAN	20.0	5.7
Ras-related protein Rab-10	P61026	RAB10_HUMAN	20.0	5.4
Dolichyl-diphosphooligosaccharide--protein glycosyltransferase subunit 1	P04843	RPN1_HUMAN	3.4	5.5
Tubulin alpha-4A chain	P68366	TBA4A_HUMAN	20.0	4.2
Very-long-chain 3-oxoacyl-CoA reductase	Q53GQ0	DHB12_HUMAN	3.5	4.2
Ras-related protein Rab-8A	P61006	RAB8A_HUMAN	20.0	5.2
Phosphate carrier protein_ mitochondrial	Q00325	MPCP_HUMAN	3.7	5.3
Transmembrane protein 33	P57088	TMM33_HUMAN	3.4	4.9
ADP-ribosylation factor 1	P84077	ARF1_HUMAN	4.4	5.4
Calnexin	P27824	CALX_HUMAN	2.1	7.2
Fructose-bisphosphate aldolase A	P04075	ALDOA_HUMAN	2.1	3.3
Apolipoprotein A-I	P02647	APOA1_HUMAN	20.0	6.5
Delta(14)-sterol reductase	Q14739	LBR_HUMAN	3.5	7.1
Sideroflexin-1	Q9H9B4	SFXN1_HUMAN	2.4	4.4
Protein kish-A	Q8TBQ9	KISHA_HUMAN	2.6	3.0
ATPase ASNA1	O43681	ASNA_HUMAN	20.0	7.5
Chitobiosyldiphosphodolichol beta-mannosyltransferase	Q9BT22	ALG1_HUMAN	3.3	4.8
Glucose-6-phosphate isomerase	P06744	G6PI_HUMAN	2.1	4.8
Plastin-2	P13796	PLSL_HUMAN	2.6	5.1
Elongation factor 1-gamma	P26641	EF1G_HUMAN	2.1	4.5
Thioredoxin-dependent peroxide reductase_ mitochondrial	P30048	PRDX3_HUMAN	20.0	4.8
Mitochondrial carrier homolog 2	Q9Y6C9	MTCH2_HUMAN	20.0	4.3
Gamma-enolase	P09104	ENOG_HUMAN	20.0	3.6
Eukaryotic initiation factor 4A-I	P60842	IF4A1_HUMAN	2.5	4.7
Dolichyl-diphosphooligosaccharide--protein glycosyltransferase 48 kDa subunit	P39656	OST48_HUMAN	3.7	4.7
Translocon-associated protein subunit delta	P51571	SSRD_HUMAN	20.0	6.0
Mitochondrial import receptor subunit TOM40 homolog	O96008	TOM40_HUMAN	20.0	1.4
ATPase family AAA domain-containing protein 3A	Q9NVI7	ATD3A_HUMAN	20.0	7.9
Dolichyl-diphosphooligosaccharide--protein glycosyltransferase subunit STT3A	P46977	STT3A_HUMAN	3.8	4.8
Dolichyl-diphosphooligosaccharide--protein glycosyltransferase subunit 2	P04844	RPN2_HUMAN	3.4	5.3
Keratin_ type II cytoskeletal 6B	P04259	K2C6B_HUMAN	20.0	2.6
Signal peptidase complex catalytic subunit SEC11A	P67812	SC11A_HUMAN	20.0	3.5
Phosphoglycerate kinase 2	P07205	PGK2_HUMAN	20.0	5.7
Vitamin K epoxide reductase complex subunit 1-like protein 1	Q8N0U8	VKORL_HUMAN	20.0	3.2
Arachidonate 5-lipoxygenase-activating protein	P20292	AL5AP_HUMAN	3.5	4.6
Inactive hydroxysteroid dehydrogenase-like protein 1	Q3SXM5	HSDL1_HUMAN	20.0	6.2
Ras-related protein Rab-14	P61106	RAB14_HUMAN	20.0	6.1
Signal recognition particle receptor subunit beta	Q9Y5M8	SRPRB_HUMAN	7.4	6.9
Estradiol 17-beta-dehydrogenase 11	Q8NBQ5	DHB11_HUMAN	4.0	4.5
14-3-3 protein beta/alpha	P31946	1433B_HUMAN	20.0	6.2
Sarcoplasmic/endoplasmic reticulum calcium ATPase 2	P16615	AT2A2_HUMAN	7.2	7.6
MICOS complex subunit MIC60	Q16891	MIC60_HUMAN	20.0	6.0
Ras-related protein Rab-30	Q15771	RAB30_HUMAN	20.0	6.4
Neutral cholesterol ester hydrolase 1	Q6PIU2	NCEH1_HUMAN	20.0	5.3
Basigin	P35613	BASI_HUMAN	2.2	5.0
Vesicular integral-membrane protein VIP36	Q12907	LMAN2_HUMAN	3.3	5.3
Lamina-associated polypeptide 2_ isoforms beta/gamma	P42167	LAP2B_HUMAN	20.0	3.9
14-3-3 protein gamma	P61981	1433G_HUMAN	2.5	1.7
Major facilitator superfamily domain-containing protein 10	Q14728	MFS10_HUMAN	2.5	3.1
Ras-related protein Rab-39A	Q14964	RB39A_HUMAN	20.0	2.4
Heterogeneous nuclear ribonucleoprotein F	P52597	HNRPF_HUMAN	2.2	3.3
NADH dehydrogenase [ubiquinone] 1 beta subcomplex subunit 4	O95168	NDUB4_HUMAN	20.0	6.1
Keratin_ type II cytoskeletal 1b	Q7Z794	K2C1B_HUMAN	20.0	2.7
Ras-related protein Rab-5C	P51148	RAB5C_HUMAN	20.0	6.6
14-3-3 protein eta	Q04917	1433F_HUMAN	20.0	2.1
OCIA domain-containing protein 1	Q9NX40	OCAD1_HUMAN	20.0	6.8
Very-long-chain enoyl-CoA reductase	Q9NZ01	TECR_HUMAN	3.8	5.4
ATP synthase subunit g_ mitochondrial	O75964	ATP5L_HUMAN	20.0	6.6
Lanosterol synthase	P48449	ERG7_HUMAN	2.4	6.3
ATP synthase subunit O_ mitochondrial	P48047	ATPO_HUMAN	20.0	1.6
Thioredoxin-related transmembrane protein 1	Q9H3N1	TMX1_HUMAN	4.0	5.1
ATP-dependent RNA helicase DDX39A	O00148	DX39A_HUMAN	20.0	7.2
Guanine nucleotide-binding protein G(i) subunit alpha-2	P04899	GNAI2_HUMAN	2.1	2.8
Histidine triad nucleotide-binding protein 3	Q9NQE9	HINT3_HUMAN	20.0	4.4
Mitochondrial import inner membrane translocase subunit TIM50	Q3ZCQ8	TIM50_HUMAN	20.0	3.8
Transmembrane emp24 domain-containing protein 10	P49755	TMEDA_HUMAN	2.1	3.1
Acyl-CoA 6-desaturase	O95864	FADS2_HUMAN	2.2	4.8
Ras-related C3 botulinum toxin substrate 2	P15153	RAC2_HUMAN	2.7	4.0
Secretory carrier-associated membrane protein 3	O14828	SCAM3_HUMAN	20.0	4.4
Extended synaptotagmin-2	A0FGR8	ESYT2_HUMAN	3.8	4.4
Sorting and assembly machinery component 50 homolog	Q9Y512	SAM50_HUMAN	20.0	4.6
Alpha-actinin-1	P12814	ACTN1_HUMAN	2.1	2.5
Equilibrative nucleoside transporter 1	Q99808	S29A1_HUMAN	20.0	4.8
Extended synaptotagmin-1	Q9BSJ8	ESYT1_HUMAN	20.0	4.9

Name	Accession	Uniprot ID	Fold-change (LEI-945/DMSO)	Significance ($-\log_{10}$)
Protein YIPF5	Q969M3	YIPF5_HUMAN	20.0	6.3
14-3-3 protein epsilon	P62258	1433E_HUMAN	3.1	3.1
Protein FAM162A	Q96A26	F162A_HUMAN	20.0	1.5
Reticulon-4	Q9NQC3	RTN4_HUMAN	20.0	3.4
NADH-cytochrome b5 reductase 3	P00387	NB5R3_HUMAN	2.1	2.3
Vesicle-associated membrane protein 8	Q9BV40	VAMP8_HUMAN	20.0	3.4
MICOS complex subunit MIC27	Q6UXV4	MIC27_HUMAN	20.0	6.2
Surfeit locus protein 4	O15260	SURF4_HUMAN	3.0	1.8
CAAX prenyl protease 1 homolog	O75844	FACE1_HUMAN	3.3	4.0
Very-long-chain (3R)-3-hydroxyacyl-CoA dehydratase 3	Q9P035	HACD3_HUMAN	3.2	4.0
Dolichyl-diphosphooligosaccharide--protein glycosyltransferase subunit STT3B	Q8TCJ2	STT3B_HUMAN	3.9	6.0
Transmembrane protein 214	Q6NUQ4	TM214_HUMAN	2.6	4.0
Ras-related protein Rab-11A	P62491	RB11A_HUMAN	20.0	2.6
Synaptogyrin-2	O43760	SNG2_HUMAN	20.0	4.9
Lysophosphatidylcholine acyltransferase 2	Q7L5N7	PCAT2_HUMAN	6.5	5.0
Protein disulfide-isomerase A6	Q15084	PDIA6_HUMAN	20.0	7.0
Translocon-associated protein subunit alpha	P43307	SSRA_HUMAN	20.0	3.8
Transmembrane protein 43	Q9BTV4	TMM43_HUMAN	3.0	3.8
Sigma non-opioid intracellular receptor 1	Q99720	SGMR1_HUMAN	20.0	4.2
Mitochondrial dicarboxylate carrier	Q9UBX3	DIC_HUMAN	20.0	1.6
Glutathione S-transferase omega-1	P78417	GSTO1_HUMAN	2.7	4.0
ADP-ribosylation factor-like protein 6-interacting protein 1	Q15041	AR6P1_HUMAN	20.0	3.5
Phosphatidylserine synthase 1	P48651	PTSS1_HUMAN	20.0	3.3
Malectin	Q14165	MLEC_HUMAN	2.4	2.9
Mitochondrial inner membrane protein OXA1L	Q15070	OXA1L_HUMAN	20.0	5.3
3-beta-hydroxysteroid-Delta(8)_Delta(7)-isomerase	Q15125	EBP_HUMAN	4.2	3.1
Translocator protein	P30536	TSPO_HUMAN	3.5	3.8
Long-chain-fatty-acid--CoA ligase 3	O95573	ACSL3_HUMAN	20.0	4.9
Catechol O-methyltransferase	P21964	COMT_HUMAN	20.0	3.8
T-complex protein 1 subunit beta	P78371	TCPB_HUMAN	2.1	3.0
Tropomyosin alpha-3 chain	P06753	TPM3_HUMAN	20.0	1.6
Carnitine O-palmitoyltransferase 1_ liver isoform	P50416	CPT1A_HUMAN	20.0	6.6
ATP-binding cassette sub-family D member 3	P28288	ABCD3_HUMAN	20.0	5.5
Cleft lip and palate transmembrane protein 1-like protein	Q96KA5	CLP1L_HUMAN	20.0	5.9
Protein transport protein Sec61 subunit alpha isoform 1	P61619	S61A1_HUMAN	4.7	4.1
B-cell receptor-associated protein 31	P51572	BAP31_HUMAN	5.5	3.2
ATP synthase F(0) complex subunit B1_ mitochondrial	P24539	AT5F1_HUMAN	2.3	4.7
Calcium load-activated calcium channel	Q9UM00	TMCO1_HUMAN	2.9	3.2
Peroxisomal biogenesis factor 3	P56589	PEX3_HUMAN	2.7	3.2
Proteasome subunit beta type-2	P49721	PSB2_HUMAN	20.0	4.9
Monocarboxylate transporter 4	O15427	MOT4_HUMAN	6.7	6.0
Calcium-binding mitochondrial carrier protein Aralar2	Q9UJS0	CMC2_HUMAN	20.0	1.5
Mitochondrial proton/calcium exchanger protein	O95202	LETM1_HUMAN	20.0	5.0
Receptor expression-enhancing protein 5	Q00765	REEP5_HUMAN	20.0	7.7
Cytochrome c oxidase subunit 2	P00403	COX2_HUMAN	2.2	2.8
RUS1 family protein C16orf58	Q96GQ5	RUS1_HUMAN	20.0	6.9
Guanine nucleotide-binding protein G(o) subunit alpha	P09471	GNAO_HUMAN	20.0	3.1
Lysocardiolipin acyltransferase 1	Q6UWP7	LCLT1_HUMAN	20.0	5.8
Protein jagunal homolog 1	Q8N5M9	JAGN1_HUMAN	20.0	6.2
Guanine nucleotide-binding protein subunit alpha-13	Q14344	GNA13_HUMAN	2.4	3.1
Sodium/potassium-transporting ATPase subunit beta-3	P54709	AT1B3_HUMAN	20.0	4.9
Myosin-10	P35580	MYH10_HUMAN	2.4	2.6
Lysosome-associated membrane glycoprotein 1	P11279	LAMP1_HUMAN	20.0	1.6
NADH dehydrogenase [ubiquinone] 1 beta subcomplex subunit 11_ mitochondrial	Q9NX14	NDUBB_HUMAN	20.0	1.6
Myosin-11	P35749	MYH11_HUMAN	8.3	4.3
Peptidyl-tRNA hydrolase 2_ mitochondrial	Q9Y3E5	PTH2_HUMAN	20.0	3.7
Thymidylate synthase	P04818	TYSY_HUMAN	20.0	7.5
Ataxin-10	Q9UBB4	ATX10_HUMAN	20.0	8.2
ATP-binding cassette sub-family B member 10_ mitochondrial	Q9NRK6	ABCBA_HUMAN	20.0	7.2
Translocation protein SEC63 homolog	Q9UGP8	SEC63_HUMAN	2.1	3.5
Myeloblastin	P24158	PRTN3_HUMAN	2.2	3.2
Vesicle-associated membrane protein-associated protein A	Q9P0L0	VAPA_HUMAN	2.9	3.0
Methylsterol monooxygenase 1	Q15800	MSMO1_HUMAN	3.4	4.8
Reticulon-3	O95197	RTN3_HUMAN	20.0	2.6
Asparagine synthetase [glutamine-hydrolyzing]	P08243	ASNS_HUMAN	5.4	5.1
Membrane-associated progesterone receptor component 1	O00264	PGRC1_HUMAN	20.0	1.6
Dol-P-Man:Man(5)GlcNAc(2)-PP-Dol alpha-1_3-mannosyltransferase	Q92685	ALG3_HUMAN	20.0	4.5
MICOS complex subunit MIC13	Q5XKP0	MIC13_HUMAN	20.0	4.1
Calcium-binding mitochondrial carrier protein Aralar1	O75746	CMC1_HUMAN	20.0	1.5
Leukocyte surface antigen CD47	Q08722	CD47_HUMAN	20.0	4.0
Receptor expression-enhancing protein 4	Q9H6H4	REEP4_HUMAN	20.0	5.9
Very long-chain acyl-CoA synthetase	O14975	S27A2_HUMAN	20.0	5.4
Importin-5	O00410	IPO5_HUMAN	2.4	3.2
Transmembrane protein 109	Q9BVC6	TM109_HUMAN	2.9	3.3
Translocation protein SEC62	Q99442	SEC62_HUMAN	3.3	3.3
Signal peptidase complex subunit 3	P61009	SPCS3_HUMAN	20.0	5.4
DNA replication licensing factor MCM6	Q14566	MCM6_HUMAN	2.4	4.4
Protein disulfide-isomerase TMX3	Q96JJ7	TMX3_HUMAN	20.0	8.2
Signal recognition particle receptor subunit alpha	P08240	SRPRA_HUMAN	2.6	3.2
4F2 cell-surface antigen heavy chain	P08195	4F2_HUMAN	20.0	6.6
Saccharopine dehydrogenase-like oxidoreductase	Q8NBX0	SCPDL_HUMAN	20.0	7.1
Myeloid-associated differentiation marker	Q96S97	MYADM_HUMAN	4.8	2.6
Tyrosine-protein kinase Lyn	P07948	LYN_HUMAN	20.0	1.6
Derlin-1	Q9BUN8	DERL1_HUMAN	20.0	5.9
Endoplasmic reticulum junction formation protein lunapark	Q9C0E8	LNP_HUMAN	20.0	1.6
Monocarboxylate transporter 1	P53985	MOT1_HUMAN	3.3	3.8
Sterol-4-alpha-carboxylate 3-dehydrogenase_ decarboxylating	Q15738	NSDHL_HUMAN	20.0	6.9

Name	Accession	Uniprot ID	Fold-change (LEI-945/DMSO)	Significance ($-\log_{10}$)
Atlastin-3	Q6DD88	ATLA3_HUMAN	20.0	5.4
Scavenger receptor class B member 1	Q8WTV0	SCRB1_HUMAN	5.2	5.4
Small ubiquitin-related modifier 1	P63165	SUMO1_HUMAN	20.0	3.4
26S proteasome non-ATPase regulatory subunit 11	O00231	PSD11_HUMAN	20.0	3.9
Neutral amino acid transporter B(0)	Q15758	AAAT_HUMAN	20.0	7.5
Long-chain-fatty-acid--CoA ligase 4	O60488	ACSL4_HUMAN	20.0	7.3
Heterogeneous nuclear ribonucleoprotein M	P52272	HNRPM_HUMAN	20.0	8.3
Minor histocompatibility antigen H13	Q8TCT9	HM13_HUMAN	20.0	1.6
Threonylcarbamoyladenosine tRNA methylthiotransferase	Q5VV42	CDKAL_HUMAN	20.0	6.3
Ras-related protein Rab-27A	P51159	RB27A_HUMAN	20.0	4.9
Endoplasmic reticulum resident protein 29	P30040	ERP29_HUMAN	20.0	1.6
Erlin-1	O75477	ERLN1_HUMAN	20.0	5.1
TraB domain-containing protein	Q9H4I3	TRABD_HUMAN	20.0	5.2
Keratin_ type I cytoskeletal 12	Q99456	K1C12_HUMAN	20.0	1.4
Basic leucine zipper and W2 domain-containing protein 1	Q7L1Q6	BZW1_HUMAN	20.0	5.0
ADP-dependent glucokinase	Q9BRR6	ADPGK_HUMAN	20.0	4.0
NADH dehydrogenase [ubiquinone] iron-sulfur protein 2_ mitochondrial	O75306	NDUS2_HUMAN	20.0	3.8
tRNA (cytosine(34)-C(5))-methyltransferase	Q08J23	NSUN2_HUMAN	20.0	6.8
Protein RFT1 homolog	Q96AA3	RFT1_HUMAN	3.5	3.9
Mitochondrial import receptor subunit TOM70	O94826	TOM70_HUMAN	20.0	1.6
Ubiquitin-associated domain-containing protein 2	Q8NBM4	UBAC2_HUMAN	20.0	5.2
NADH-ubiquinone oxidoreductase chain 5	P03915	NU5M_HUMAN	20.0	4.8
Vesicle-associated membrane protein 7	P51809	VAMP7_HUMAN	20.0	4.6
Protein ERGIC-53	P49257	LMAN1_HUMAN	20.0	4.2
Nicalin	Q969V3	NCLN_HUMAN	20.0	5.1
Choline/ethanolaminephosphotransferase 1	Q9Y6K0	CEPT1_HUMAN	20.0	6.7
Peptidyl-prolyl cis-trans isomerase FKBP8	Q14318	FKBP8_HUMAN	20.0	5.9
DnaJ homolog subfamily C member 11	Q9NVH1	DJC11_HUMAN	20.0	6.2
Squalene synthase	P37268	FDFT_HUMAN	20.0	5.4
Sorbitol dehydrogenase	Q00796	DHSO_HUMAN	20.0	7.0
Thioredoxin domain-containing protein 5	Q8NBS9	TXND5_HUMAN	20.0	7.5
CDGSH iron-sulfur domain-containing protein 2	Q8N5K1	CISD2_HUMAN	20.0	4.5
Signal recognition particle subunit SRP68	Q9UHB9	SRP68_HUMAN	20.0	5.4
Retinol dehydrogenase 11	Q8TC12	RDH11_HUMAN	20.0	4.6
Cation-dependent mannose-6-phosphate receptor	P20645	MPRD_HUMAN	20.0	4.5
GPI-anchor transamidase	Q92643	GPI8_HUMAN	20.0	1.6
Heat shock 70 kDa protein 4	P34932	HSP74_HUMAN	2.1	3.4
Adenosine 3'-phospho 5'-phosphosulfate transporter 1	Q8TB61	S35B2_HUMAN	20.0	4.3
GDP-Man:Man(3)GlcNAc(2)-PP-Dol alpha-1_2-mannosyltransferase	Q2TAA5	ALG11_HUMAN	20.0	4.9
Phosphatidylinositol glycan anchor biosynthesis class U protein	Q9H490	PIGU_HUMAN	2.9	2.7
Spermidine synthase	P19623	SPEE_HUMAN	20.0	1.6
Heme oxygenase 2	P30519	HMOX2_HUMAN	20.0	5.5
Exportin-2	P55060	XPO2_HUMAN	2.0	4.5
Solute carrier family 43 member 3	Q8NBI5	S43A3_HUMAN	20.0	5.5
Cytochrome c-type heme lyase	P53701	CCHL_HUMAN	20.0	1.6
Fatty aldehyde dehydrogenase	P51648	AL3A2_HUMAN	20.0	6.4
ATP-dependent 6-phosphofructokinase_ liver type	P17858	PFKAL_HUMAN	20.0	8.0
Sigma intracellular receptor 2	Q5BJF2	SGMR2_HUMAN	20.0	2.4
Sarcoplasmic/endoplasmic reticulum calcium ATPase 3	Q93084	AT2A3_HUMAN	20.0	7.0
Large neutral amino acids transporter small subunit 1	Q01650	LAT1_HUMAN	20.0	6.4
Kelch-like ECH-associated protein 1	Q14145	KEAP1_HUMAN	20.0	6.5
Long-chain-fatty-acid--CoA ligase 1	P33121	ACSL1_HUMAN	20.0	5.4
PCI domain-containing protein 2	Q5JVF3	PCID2_HUMAN	20.0	1.6
FAS-associated factor 2	Q96CS3	FAF2_HUMAN	20.0	5.1
Glycine--tRNA ligase	P41250	GARS_HUMAN	20.0	3.2
Sphingomyelin phosphodiesterase 4	Q9NXE4	NSMA3_HUMAN	20.0	6.9
Protein SET	Q01105	SET_HUMAN	20.0	6.1

Supplementary Table 7.3 | Proteins significantly enriched by STA-211 (10 µM) in A549 cells corresponding to Fig. 7.5c.

Name	Accession	Uniprot ID	Fold change (UV/EtOH)	Significance ($-\log_{10}$)	UV enriched
15-hydroxyprostaglandin dehydrogenase [NAD(+)]	P15428	PGDH_HUMAN	20.0	1.5	Yes
Keratin_ type II cytoskeletal 1b	Q7Z794	K2C1B_HUMAN	20.0	2.2	Yes
Keratin_ type I cytoskeletal 17	Q04695	K1C17_HUMAN	20.0	3.3	Yes
Neutral cholesterol ester hydrolase 1	Q6PIU2	NCEH1_HUMAN	20.0	2.1	Yes
ATPase ASNA1	O43681	ASNA_HUMAN	20.0	1.6	Yes
Magnesium transporter protein 1	Q9H0U3	MAGT1_HUMAN	20	4.8	Yes
Epoxide hydrolase 1	P07099	HYEP_HUMAN	4.0	2.8	Yes
Ras-related protein Rab-10	P61026	RAB10_HUMAN	20.0	5	No
Fatty aldehyde dehydrogenase	P51648	AL3A2_HUMAN	20.0	4.3	No
Ras-related protein Rab-1A	P62820	RAB1A_HUMAN	20.0	4.6	No
Alpha-actinin-1	P12814	ACTN1_HUMAN	20.0	3.2	No
14-3-3 protein theta	P27348	1433T_HUMAN	20.0	4	No
Vimentin	P08670	VIME_HUMAN	20.0	5.1	No
Voltage-dependent anion-selective channel protein 3	Q9Y277	VDAC3_HUMAN	20.0	4.1	No
14-3-3 protein gamma	P61981	1433G_HUMAN	20.0	4.7	No
14-3-3 protein beta/alpha	P31946	1433B_HUMAN	20.0	3.5	No
Keratin_ type II cytoskeletal 7	P08729	K2C7_HUMAN	20.0	4.7	No
Tubulin beta-4B chain	P68371	TBB4B_HUMAN	20.0	5.5	No
Tubulin alpha-4A chain	P68366	TBA4A_HUMAN	20.0	5.5	No
Dolichyl-diphosphooligosaccharide--protein glycosyltransferase subunit DAD1	P61803	DAD1_HUMAN	20.0	3.7	No
14-3-3 protein epsilon	P62258	1433E_HUMAN	20.0	3.6	No
Microsomal glutathione S-transferase 3	O14880	MGST3_HUMAN	20.0	2.7	No
Poly(rC)-binding protein 1	Q15365	PCBP1_HUMAN	20.0	4.9	No
Poly(rC)-binding protein 2	Q15366	PCBP2_HUMAN	20.0	3.4	No
Cytochrome b5 type B	O43169	CYB5B_HUMAN	20.0	2.8	No
ATP synthase subunit alpha_ mitochondrial	P25705	ATPA_HUMAN	20.0	4.1	No
Keratin_ type I cytoskeletal 13	P13646	K1C13_HUMAN	20.0	3.1	No
Prohibitin-2	Q99623	PHB2_HUMAN	20.0	3.2	No
Heat shock 70 kDa protein 1A	P0DMV8	HS71A_HUMAN	20.0	5	No
Prohibitin	P35232	PHB_HUMAN	20.0	3.6	No
Keratin_ type I cytoskeletal 19	P08727	K1C19_HUMAN	20.0	5.9	No
Keratin_ type II cytoskeletal 75	O95678	K2C75_HUMAN	20.0	3.5	No
Sulfide:quinone oxidoreductase_ mitochondrial	Q9Y6N5	SQOR_HUMAN	20.0	5	No
Sideroflexin-1	Q9H9B4	SFXN1_HUMAN	20.0	3.6	No
40S ribosomal protein S3	P23396	RS3_HUMAN	20.0	4.5	No
Mitochondrial import inner membrane translocase subunit TIM50	Q3ZCQ8	TIM50_HUMAN	20.0	1.6	No
40S ribosomal protein S20	P60866	RS20_HUMAN	20.0	3.1	No
Putative heat shock protein HSP 90-beta 2	Q58FF8	H90B2_HUMAN	20.0	3.5	No
Trifunctional enzyme subunit beta_ mitochondrial	P55084	ECHB_HUMAN	20.0	6	No
78 kDa glucose-regulated protein	P11021	BIP_HUMAN	20.0	5	No
ADP-ribosylation factor 1	P84077	ARF1_HUMAN	20.0	4.3	No
Ubiquitin carboxyl-terminal hydrolase isozyme L1	P09936	UCHL1_HUMAN	20.0	3.8	No
Mitochondrial import receptor subunit TOM40 homolog	O96008	TOM40_HUMAN	20.0	3.1	No
Dolichyl-diphosphooligosaccharide--protein glycosyltransferase subunit 1	P04843	RPN1_HUMAN	20.0	3.1	No
Very-long-chain (3R)-3-hydroxyacyl-CoA dehydratase	H3BPZ1	H3BPZ1_HUMAN	20.0	2.4	No
Thioredoxin-related transmembrane protein 1	Q9H3N1	TMX1_HUMAN	20.0	3.9	No
Protein transport protein Sec61 subunit alpha isoform 1	P61619	S61A1_HUMAN	20.0	4.3	No
Nucleophosmin	P06748	NPM_HUMAN	20.0	3.8	No
Aldehyde dehydrogenase_ mitochondrial	P05091	ALDH2_HUMAN	20.0	5.1	No
Glutathione S-transferase P	P09211	GSTP1_HUMAN	20.0	4.2	No
40S ribosomal protein S16	P62249	RS16_HUMAN	20.0	3.5	No
Rho-related GTP-binding protein RhoC	P08134	RHOC_HUMAN	20.0	4.8	No
60S ribosomal protein L11	P62913	RL11_HUMAN	20.0	3.7	No
Phosphoglycerate kinase 1	P00558	PGK1_HUMAN	20.0	6.5	No
ATP-dependent 6-phosphofructokinase_ platelet type	Q01813	PFKAP_HUMAN	20.0	3.4	No
60S acidic ribosomal protein P0	P05388	RLA0_HUMAN	20.0	3.3	No
Malate dehydrogenase_ mitochondrial	P40926	MDHM_HUMAN	20.0	5	No
PRA1 family protein 2	O60831	PRAF2_HUMAN	20.0	2.9	No
Keratin_ type I cuticular Ha1	Q15323	K1H1_HUMAN	20.0	8.3	No
Tetraspanin	P48509	CD151_HUMAN	20.0	2.3	No
Leucine-rich repeat-containing protein 59	Q96AG4	LRC59_HUMAN	20.0	5.2	No
Ezrin	P15311	EZRI_HUMAN	20.0	2.4	No
Estradiol 17-beta-dehydrogenase 11	Q8NBQ5	DHB11_HUMAN	20.0	3.6	No
Malate dehydrogenase_ cytoplasmic	P40925	MDHC_HUMAN	20.0	4.6	No
Trifunctional enzyme subunit alpha_ mitochondrial	P40939	ECHA_HUMAN	20.0	4.6	No
Carnitine O-palmitoyltransferase 1_ liver isoform	P50416	CPT1A_HUMAN	20.0	1.6	No
Stress-70 protein_ mitochondrial	P38646	GRP75_HUMAN	20.0	8.4	No
Minor histocompatibility antigen H13	Q8TCT9	HM13_HUMAN	20.0	2.8	No
Synaptogyrin-2	O43760	SNG2_HUMAN	20.0	1.5	No
Ras-related C3 botulinum toxin substrate 2	P15153	RAC2_HUMAN	20.0	6.1	No
Filamin-A	P21333	FLNA_HUMAN	20.0	5	No
60S ribosomal protein L5	P46777	RL5_HUMAN	20.0	3.1	No
Isocitrate dehydrogenase [NADP] cytoplasmic	O75874	IDHC_HUMAN	20.0	6.6	No
Transgelin-2	P37802	TAGL2_HUMAN	20.0	3	No
Heterogeneous nuclear ribonucleoprotein K	P61978	HNRPK_HUMAN	20.0	4.6	No
Destrin	P60981	DEST_HUMAN	20.0	4.1	No
40S ribosomal protein SA	P08865	RSSA_HUMAN	20.0	5.4	No
Tetraspanin	P21926	CD9_HUMAN	20.0	5.1	No
Keratin-like protein KRT222	Q8N1A0	KT222_HUMAN	20.0	2.2	No
Heterogeneous nuclear ribonucleoprotein A1	P09651	ROA1_HUMAN	20.0	4.9	No
Nucleolin	P19338	NUCL_HUMAN	20.0	7.3	No
60S ribosomal protein L12	P30050	RL12_HUMAN	20.0	3.8	No
Importin subunit beta-1	Q14974	IMB1_HUMAN	20.0	3.9	No
Bifunctional purine biosynthesis protein PURH	P31939	PUR9_HUMAN	20.0	4.7	No
Thioredoxin-related transmembrane protein 2	Q9Y320	TMX2_HUMAN	20.0	4.5	No
Dehydrogenase/reductase SDR family member 7	Q9Y394	DHRS7_HUMAN	20.0	1.5	No
Thioredoxin	P10599	THIO_HUMAN	20.0	3.9	No
Glutathione reductase_ mitochondrial	P00390	GSHR_HUMAN	20.0	4.4	No
Ras-related protein Rab-11A	P62491	RB11A_HUMAN	20.0	5.1	No
Adenosylhomocysteinase	P23526	SAHH_HUMAN	20.0	2.9	No

Name	Accession	Uniprot ID	Fold change (UV/EtOH)	Significance ($-\log_{10}$)	UV enriched
B-cell receptor-associated protein 31	P51572	BAP31_HUMAN	20.0	7.6	No
ADP-ribosylation factor 4	P18085	ARF4_HUMAN	20.0	1.6	No
Isoform 4 of Filamin-B	O75369-4	FLNB_HUMAN	20.0	3.4	No
Glutathione S-transferase omega-1	P78417	GSTO1_HUMAN	20.0	6.2	No
Leucine-rich PPR motif-containing protein_ mitochondrial	P42704	LPPRC_HUMAN	20.0	7.1	No
Stress-induced-phosphoprotein 1	P31948	STIP1_HUMAN	20.0	8	No
Dolichyl-diphosphooligosaccharide--protein glycosyltransferase subunit 2	P04844	RPN2_HUMAN	20.0	4.5	No
Elongation factor 1-gamma	P26641	EF1G_HUMAN	20.0	4.8	No
Glycogen phosphorylase_ brain form	P11216	PYGB_HUMAN	20.0	4.5	No
Long-chain-fatty-acid--CoA ligase 3	O95573	ACSL3_HUMAN	20.0	1.4	No
Prenylcysteine oxidase 1	Q9UHG3	PCYOX_HUMAN	20.0	2.6	No
Lamin-B receptor	Q14739	LBR_HUMAN	20.0	4	No
Sodium/potassium-transporting ATPase subunit alpha-1	P05023	AT1A1_HUMAN	20.0	1.5	No
60S ribosomal protein L26	P61254	RL26_HUMAN	20.0	4	No
Protein disulfide-isomerase A3	P30101	PDIA3_HUMAN	20.0	4.6	No
Very-long-chain enoyl-CoA reductase	Q9NZ01	TECR_HUMAN	20.0	3.8	No
Myosin-9	P35579	MYH9_HUMAN	20.0	3	No
Alpha-1_3-glucosyltransferase	Q9BVK2	ALG8_HUMAN	20.0	1.5	No
Vesicular integral-membrane protein VIP36	Q12907	LMAN2_HUMAN	20.0	1.6	No
Lysophospholipid acyltransferase 7	Q96N66	MBOA7_HUMAN	20.0	4.5	No
ATP synthase membrane subunit g	O75964	ATP5L_HUMAN	20.0	1.6	No
Tricarboxylate transport protein_ mitochondrial	P53007	TXTP_HUMAN	20.0	1.6	No
Mitochondrial inner membrane protein OXA1L	Q15070	OXA1L_HUMAN	20.0	1.5	No
T-complex protein 1 subunit theta	P50990	TCPQ_HUMAN	20.0	1.6	No
Adipocyte plasma membrane-associated protein	Q9HDC9	APMAP_HUMAN	20.0	3.1	No
Protein disulfide-isomerase A4	P13667	PDIA4_HUMAN	20.0	5.6	No
Elongation factor Tu_ mitochondrial	P49411	EFTU_HUMAN	20.0	5.8	No
ATP-binding cassette sub-family D member 3	P28288	ABCD3_HUMAN	20.0	6.4	No
Aspartate aminotransferase_ mitochondrial	P00505	AATM_HUMAN	20.0	5.6	No
Chloride intracellular channel protein 1	O00299	CLIC1_HUMAN	20.0	1.6	No
Serum albumin	P02768	ALBU_HUMAN	20.0	1.4	No
Mitochondrial import receptor subunit TOM20 homolog	Q15388	TOM20_HUMAN	20.0	1.6	No
Splicing factor_ proline- and glutamine-rich	P23246	SFPQ_HUMAN	20.0	3.1	No
T-complex protein 1 subunit beta	P78371	TCPB_HUMAN	20	6.2	No
Endoplasmic reticulum metallopeptidase 1	Q7Z2K6	ERMP1_HUMAN	20	1.6	No
Cytoskeleton-associated protein 4	Q07065	CKAP4_HUMAN	20	1.6	No
Elongation of very long chain fatty acids protein 1	Q9BW60	ELOV1_HUMAN	20	1.6	No
Filamin-A	P21333	FLNA_HUMAN	20	6.3	No
X-ray repair cross-complementing protein 6	P12956	XRCC6_HUMAN	20	3.8	No
T-complex protein 1 subunit delta	P50991	TCPD_HUMAN	20	4.6	No
Spectrin beta chain_ non-erythrocytic 1	Q01082	SPTB2_HUMAN	20	1.5	No
C-1-tetrahydrofolate synthase_ cytoplasmic	P11586	C1TC_HUMAN	20	2.3	No
ATP-dependent RNA helicase A	Q08211	DHX9_HUMAN	20	4	No
ADP/ATP translocase 2	P05141	ADT2_HUMAN	11.3	3.5	No
Voltage-dependent anion-selective channel protein 2	P45880	VDAC2_HUMAN	9.0	3	No
Aldo-keto reductase family 1 member C3	P42330	AK1C3_HUMAN	7.1	4	No
Keratin_ type II cuticular Hb1	Q14533	KRT81_HUMAN	7.0	4.2	No
Heat shock protein HSP 90-beta	P08238	HS90B_HUMAN	5.9	3.7	No
Keratin_ type II cytoskeletal 8	P05787	K2C8_HUMAN	5.8	3.7	No
Glyceraldehyde-3-phosphate dehydrogenase	P04406	G3P_HUMAN	5.7	3.9	No
Aldo-keto reductase family 1 member B10	O60218	AK1BA_HUMAN	5.6	4.9	No
Aldo-keto reductase family 1 member C2	P52895	AK1C2_HUMAN	5.6	3.7	No
Phosphate carrier protein_ mitochondrial	Q00325	MPCP_HUMAN	5.6	3.3	No
Retinal dehydrogenase 1	P00352	AL1A1_HUMAN	5.0	4.8	No
Voltage-dependent anion-selective channel protein 1	P21796	VDAC1_HUMAN	4.9	2.3	No
Annexin A1	P04083	ANXA1_HUMAN	4.7	3.7	No
Large neutral amino acids transporter small subunit 1	Q01650	LAT1_HUMAN	4.6	3.1	No
Keratin_ type I cytoskeletal 18	P05783	K1C18_HUMAN	4.4	3	No
L-lactate dehydrogenase A chain	P00338	LDHA_HUMAN	4.1	3.2	No
L-lactate dehydrogenase B chain	P07195	LDHB_HUMAN	4.0	3.4	No
Elongation factor 1-alpha 1	P68104	EF1A1_HUMAN	4.0	3.2	No
Peroxiredoxin-1	Q06830	PRDX1_HUMAN	3.6	3.2	No
NAD(P)H dehydrogenase [quinone] 1	P15559	NQO1_HUMAN	3.5	3	No
Fructose-bisphosphate aldolase A	P04075	ALDOA_HUMAN	3.4	3.5	No
Tubulin alpha-1A chain	Q71U36	TBA1A_HUMAN	3.3	3.1	No
Pyruvate kinase PKM	P14618	KPYM_HUMAN	3.2	4.2	No
Alpha-actinin-4	O43707	ACTN4_HUMAN	3.2	2.5	No
Elongation factor 2	P13639	EF2_HUMAN	3.2	3.1	No
6-phosphogluconate dehydrogenase_ decarboxylating	P52209	6PGD_HUMAN	3.1	2.5	No
Tubulin beta chain	P04350	TBB4A_HUMAN	3.1	3.1	No
Aldehyde dehydrogenase_ dimeric NADP-preferring	P30838	AL3A1_HUMAN	3.0	3.5	No
Alpha-enolase	P06733	ENOA_HUMAN	2.9	3	No
Sarcoplasmic/endoplasmic reticulum calcium ATPase 2	P16615	AT2A2_HUMAN	2.9	3.1	No
Profilin-1	P07737	PROF1_HUMAN	2.8	3.4	No
Endoplasmin	P14625	ENPL_HUMAN	2.8	3.2	No
ADP/ATP translocase 3	P12236	ADT3_HUMAN	2.7	2.4	No
Protein S100	P06703	S10A6_HUMAN	2.7	3	No
Heat shock protein HSP 90-alpha	P07900	HS90A_HUMAN	2.5	2.2	No
Histone H1.2	P16403	H12_HUMAN	2.5	3	No
Actin_ cytoplasmic 1	P60709	ACTB_HUMAN	2.4	2.2	No
Polyubiquitin-B	P0CG47	UBB_HUMAN	2.4	2.7	No
Transketolase	P29401	TKT_HUMAN	2.4	1.8	No
Putative heat shock protein HSP 90-beta-3	Q58FF7	H90B3_HUMAN	2.4	2.5	No
60S ribosomal protein L27a	P46776	RL27A_HUMAN	2.3	2.6	No
Cofilin 1 (Non-muscle)_ isoform CRA_a	G3V1A4	G3V1A4_HUMAN	2.3	2.3	No
60 kDa heat shock protein_ mitochondrial	P10809	CH60_HUMAN	2.3	2.8	No
60S ribosomal protein L6	Q02878	RL6_HUMAN	2.3	2.3	No
Glucose-6-phosphate isomerase	Q92643	GPI8_HUMAN	2.2	2.1	No
Heterogeneous nuclear ribonucleoproteins A2/B1	P22626	ROA2_HUMAN	2.2	2.5	No
60S ribosomal protein L7a	P62424	RL7A_HUMAN	2.2	2.4	No
14-3-3 protein zeta/delta	P63104	1433Z_HUMAN	2.1	2.2	No
Nicotinamide phosphoribosyltransferase	P43490	NAMPT_HUMAN	2.1	2.6	No
40S ribosomal protein S8	P62241	RS8_HUMAN	2.1	2.2	No
ATP-citrate synthase	P53396	ACLY_HUMAN	2.1	2.8	No

Supplementary Table 7.4 | Proteins significantly enriched by STA-215 (10 µM) in A549 cells corresponding to Fig. 7.5d.

Name	Accession	Uniprot ID	Fold-change (UV/EtOH)	Significance ($-\log_{10}$)	UV enriched
Endoplasmin	P14625	ENPL_HUMAN	20.0	2.7	Yes
Voltage-dependent anion-selective channel protein 1	P21796	VDAC1_HUMAN	20.0	2.9	Yes
Vesicular integral-membrane protein VIP36	Q12907	LMAN2_HUMAN	20.0	3.7	Yes
Neutral cholesterol ester hydrolase 1	Q6PIU2	NCEH1_HUMAN	20.0	4.0	Yes
Prohibitin-2	Q99623	PHB2_HUMAN	20.0	2.7	Yes
Adipocyte plasma membrane-associated protein	Q9HDC9	APMAP_HUMAN	20.0	3.4	Yes
Mitochondrial import inner membrane translocase subunit TIM50	Q3ZCQ8	TIM50_HUMAN	20.0	1.5	Yes
Voltage-dependent anion-selective channel protein 3	Q9Y277	VDAC3_HUMAN	20.0	1.7	Yes
ATPase ASNA1	O43681	ASNA_HUMAN	20.0	4.0	Yes
Cleft lip and palate transmembrane protein 1	O96005	CLPT1_HUMAN	20.0	3.6	Yes
Leucine-rich repeat-containing protein 59	Q96AG4	LRC59_HUMAN	20.0	3.6	Yes
NADH dehydrogenase [ubiquinone] 1 alpha subcomplex subunit 10_ mitochondrial	O95299	NDUAA_HUMAN	20.0	2.0	Yes
ADP/ATP translocase 2	P05141	ADT2_HUMAN	17.3	2.2	Yes
Phosphate carrier protein_ mitochondrial	Q00325	MPCP_HUMAN	12.7	3.3	Yes
Aldo-keto reductase family 1 member C2	P52895	AK1C2_HUMAN	10.3	3.8	Yes
ADP/ATP translocase 1	P12235	ADT1_HUMAN	10.0	1.9	Yes
Epoxide hydrolase 1	P07099	HYEP_HUMAN	8.8	4.1	Yes
Voltage-dependent anion-selective channel protein 2	P45880	VDAC2_HUMAN	8.0	2.4	Yes
Transgelin-2	P37802	TAGL2_HUMAN	20.0	11.2	No
Protein S100	P06703	S10A6_HUMAN	20.0	4.6	No
Sarcoplasmic/endoplasmic reticulum calcium ATPase 2	P16615	AT2A2_HUMAN	20.0	3.1	No
Serum albumin	P02768	ALBU_HUMAN	20.0	4.3	No
Rab GDP dissociation inhibitor beta	P50395	GDIB_HUMAN	20.0	5.0	No
Isocitrate dehydrogenase [NADP] cytoplasmic	O75874	IDHC_HUMAN	20.0	3.8	No
Keratin_ type II cytoskeletal 7	P08729	K2C7_HUMAN	20.0	4.0	No
Chloride intracellular channel protein 1	O00299	CLIC1_HUMAN	20.0	3.3	No
Elongation factor 1-gamma	P26641	EF1G_HUMAN	20.0	5.2	No
40S ribosomal protein SA	P08865	RSSA_HUMAN	20.0	4.8	No
Stress-70 protein_ mitochondrial	P38646	GRP75_HUMAN	20.0	4.7	No
Phosphoglycerate kinase 1	P00558	PGK1_HUMAN	20.0	9.4	No
Isoform 4 of Filamin-B	O75369-4	FLNB_HUMAN	20.0	4.3	No
Transaldolase	P37837	TALDO_HUMAN	20.0	4.8	No
Protein disulfide-isomerase	P07237	PDIA1_HUMAN	20.0	5.4	No
Leucine-rich PPR motif-containing protein_ mitochondrial	P42704	LPPRC_HUMAN	20.0	6.8	No
Ubiquitin carboxyl-terminal hydrolase	P09936	UCHL1_HUMAN	20.0	3.2	No
Sideroflexin-1	Q9H9B4	SFXN1_HUMAN	20.0	3.1	No
15-hydroxyprostaglandin dehydrogenase [NAD(+)]	P15428	PGDH_HUMAN	20.0	7.8	No
Trifunctional enzyme subunit alpha_ mitochondrial	P40939	ECHA_HUMAN	20.0	1.8	No
4F2 cell-surface antigen heavy chain	P08195	4F2_HUMAN	20.0	7.2	No
Putative keratin-87 protein	A6NCN2	KR87P_HUMAN	20.0	3.3	No
Protein disulfide-isomerase A4	P13667	PDIA4_HUMAN	20.0	6.0	No
78 kDa glucose-regulated protein	P11021	BIP_HUMAN	20.0	7.3	No
Large neutral amino acids transporter small subunit 1	Q01650	LAT1_HUMAN	8.5	2.9	No
Aldo-keto reductase family 1 member C3	P42330	AK1C3_HUMAN	7.7	2.7	No
Aldo-keto reductase family 1 member B10	O60218	AK1BA_HUMAN	7.0	2.8	No
14-3-3 protein zeta/delta	P63104	1433Z_HUMAN	5.5	2.6	No
Heat shock protein HSP 90-alpha	P07900	HS90A_HUMAN	4.6	2.9	No
Retinal dehydrogenase 1	P00352	AL1A1_HUMAN	4.5	2.6	No
Annexin A1	P04083	ANXA1_HUMAN	4.4	2.4	No
Elongation factor 1-alpha 1	P68104	EF1A1_HUMAN	4.0	2.6	No
Polyubiquitin-B	P0CG47	UBB_HUMAN	4.0	2.3	No
Heat shock cognate 71 kDa protein	P11142	HSP7C_HUMAN	3.6	2.5	No
L-lactate dehydrogenase B chain	P07195	LDHB_HUMAN	3.5	1.9	No
UDP-glucose 6-dehydrogenase	O60701	UGDH_HUMAN	3.5	2.4	No
Annexin A2	P07355	ANXA2_HUMAN	3.5	2.6	No
Heat shock protein HSP 90-beta	P08238	HS90B_HUMAN	3.3	2.6	No
L-lactate dehydrogenase A chain	P00338	LDHA_HUMAN	3.3	2.0	No
Vimentin	P08670	VIME_HUMAN	3.3	2.5	No
Alpha-enolase	P06733	ENOA_HUMAN	3.3	1.9	No
14-3-3 protein theta	P27348	1433T_HUMAN	3.2	2.5	No
Keratin_ type I cytoskeletal 18	P05783	K1C18_HUMAN	3.2	1.7	No
Aldose reductase	P15121	ALDR_HUMAN	3.1	1.7	No
Heat shock 70 kDa protein 1A	P0DMV8	HS71A_HUMAN	3.0	2.3	No
Pyruvate kinase PKM	P14618	KPYM_HUMAN	2.9	1.7	No
Glucose-6-phosphate 1-dehydrogenase	P11413	G6PD_HUMAN	2.9	1.8	No
Fructose-bisphosphate aldolase A	P04075	ALDOA_HUMAN	2.8	1.6	No
Elongation factor 2	P13639	EF2_HUMAN	2.8	2.1	No
Keratin_ type II cytoskeletal 8	P05787	K2C8_HUMAN	2.7	2.0	No
Triosephosphate isomerase	P60174	TPIS_HUMAN	2.7	2.1	No
Actin_ cytoplasmic 1	P60709	ACTB_HUMAN	2.6	1.6	No
Aldehyde dehydrogenase_ dimeric NADP-preferring	P30838	AL3A1_HUMAN	2.5	1.8	No
Filamin-A	P21333	FLNA_HUMAN	2.5	2.4	No
Tubulin beta chain	P04350	TBB4A_HUMAN	2.5	1.5	No
Glutathione reductase_ mitochondrial	P00390	GSHR_HUMAN	2.5	2.3	No
Transketolase	P29401	TKT_HUMAN	2.4	2.1	No
Nicotinamide phosphoribosyltransferase	P43490	NAMPT_HUMAN	2.4	1.9	No
Profilin-1	P07737	PROF1_HUMAN	2.3	1.8	No
Tubulin alpha-1C chain	Q9BQE3	TBA1C_HUMAN	2.1	1.9	No
Glutathione S-transferase P	P09211	GSTP1_HUMAN	2.1	2.0	No

References

1. Haberkant, P. & Holthuis, J. C. M. Fat & fabulous: Bifunctional lipids in the spotlight. *Biochim. Biophys. Acta - Mol. Cell Biol. Lipids* **1841**, 1022–1030 (2014).
2. Thiele, C. *et al.* Tracing fatty acid metabolism by click chemistry. *ACS Chem. Biol.* **7**, 2004–2011 (2012).
3. Robichaud, P. P. *et al.* On the cellular metabolism of the click chemistry probe 19-alkyne arachidonic acid. *J. Lipid Res.* **57**, 1821–1830 (2016).
4. Gaebler, A. *et al.* Alkyne lipids as substrates for click chemistry-based in vitro enzymatic assays. *J. Lipid Res.* **54**, 2282–2290 (2013).
5. Hannoush, R. N. & Arenas-Ramirez, N. Imaging the lipidome: ω-alkynyl fatty acids for detection and cellular visualization of lipid-modified proteins. *ACS Chem. Biol.* **4**, 581–587 (2009).
6. Heal, W. P., Wickramasinghe, S. R., Leatherbarrow, R. J. & Tate, E. W. N-Myristoyl transferase-mediated protein labelling in vivo. *Org. Biomol. Chem.* **6**, 2308–2315 (2008).
7. Hang, H. C. *et al.* Chemical probes for the rapid detection of fatty-acylated proteins in mammalian cells. *J. Am. Chem. Soc.* **129**, 2744–2745 (2007).
8. Koenders, S. T. A. *et al.* Development of a Retinal-Based Probe for the Profiling of Retinaldehyde Dehydrogenases in Cancer Cells. *ACS Cent. Sci.* **5**, 1965–1974 (2019).
9. Budhu, A. S. & Noy, N. Direct channeling of retinoic acid between cellular retinoic acid-binding protein II and retinoic acid receptor sensitizes mammary carcinoma cells to retinoic acid-induced growth arrest. *Mol. Cell. Biol.* **22**, 2632–41 (2002).
10. Erkelens, M. N. & Mebius, R. E. Retinoic Acid and Immune Homeostasis: A Balancing Act. *Trends in Immunology* **38**, 168–180 (2017).
11. Kleiner, P., Heydenreuter, W., Stahl, M., Korotkov, V. S. & Sieber, S. A. A Whole Proteome Inventory of Background Photocrosslinker Binding. *Angew. Chemie Int. Ed.* **56**, 1396–1401 (2017).
12. Murayama, A., Suzuki, T. & Matsui, M. Photoisomerization of retinoic acids in ethanol under room light: A warning for cell biological study of geometrical isomers of retinoids. *J. Nutr. Sci. Vitaminol. (Tokyo).* **43**, 167–176 (1997).
13. Kiser, P. D., Golczak, M. & Palczewski, K. Chemistry of the retinoid (visual) cycle. *Chem. Rev.* **114**, 194–232 (2014).
14. Dillon, J., Gaillard, E. R., Bilski, P., Chignell, C. F. & Reszka, K. J. The photochemistry of the retinoids as studied by steady-state and pulsed methods. *Photochem. Photobiol.* **63**, 680–685 (1996).
15. Lo, K. K. N., Land, E. J. & TRUSCOTT, T. G. PRIMARY INTERMEDIATES IN THE PULSED IRRADIATION OF RETINOIDS. *Photochem. Photobiol.* **36**, 139–145 (1982).
16. Bayley, H. & Knowles, J. R. Photoaffinity labeling. *Methods Enzymol.* **46**, 69–114 (1977).
17. Bernstein, P. S., Choi, S. Y., Ho, Y. C. & Rando, R. R. Photoaffinity labeling of retinoic acid-binding proteins. *Proc. Natl. Acad. Sci. U. S. A.* **92**, 654–658 (1995).
18. Chen, G. & Radominska-Pandya, A. Direct photoaffinity labeling of cellular retinoic acid-binding protein I (CRABP-I) with all-trans-retinoic acid: Identification of amino acids in the ligand binding site. *Biochemistry* **39**, 12568–12574 (2000).
19. Radominska-Pandya, A. & Chen, G. Photoaffinity labeling of human retinoid X receptor β (RXRβ) with 9-cis-retinoic acid: Identification of phytanic acid, docosahexaenoic acid, and lithocholic acid as ligands for RXRβ. *Biochemistry* **41**, 4883–4890 (2002).
20. Lambertin, F., Wende, M., Quirin, M. J., Taran, M. & Delmond, B. New retinoid analogs from δ-pyronene, a natural synthon. *European J. Org. Chem.* **1999**, 1489–1494 (1999).
21. Birnie, G. D. The HL60 cell line: a model system for studying human myeloid cell differentiation. *Br. J. Cancer. Suppl.* **9**, 41–5 (1988).
22. Miller, L. J., Bainton, D. F., Borregaard, N. & Springer, T. A. Stimulated mobilization of monocyte Mac-1 and p150,95 adhesion proteins from an intracellular vesicular compartment to the cell surface. *J. Clin. Invest.* **80**, 535–544 (1987).
23. Napoli, J. L. Cellular retinoid binding-proteins, CRBP, CRABP, FABP5: Effects on retinoid metabolism, function and related diseases. *Pharmacology and Therapeutics* **173**, 19–33 (2017).
24. Huang, D. W., Sherman, B. T. & Lempicki, R. A. Systematic and integrative analysis of large gene lists using DAVID bioinformatics resources. *Nat. Protoc.* **4**, 44–57 (2009).
25. Ogata, H., Goto, S., Fujibuchi, W. & Kanehisa, M. Computation with the KEGG pathway database. *Biosystems* **47**, 119–128 (1998).

26. Thomas, P. D. *et al.* PANTHER: A browsable database of gene products organized by biological function, using curated protein family and subfamily classification. *Nucleic Acids Research* **31**, 334–341 (2003).
27. McGrath, K. E., Bushnell, T. P. & Palis, J. Multispectral imaging of hematopoietic cells: Where flow meets morphology. *J. Immunol. Methods* **336**, 91–97 (2008).
28. Barua, A. B. & Furr, H. C. Properties of retinoids. Structure, handling, and preparation. *Applied Biochemistry and Biotechnology - Part B Molecular Biotechnology* **10**, 167–182 (1998).
29. Babler, J. H., Coghlan, M. J., Feng, M. & Fries, P. Facile Synthesis of 4-Acetoxy-2-methyl-2-butenal, a Vitamin A Precursor, from Isoprene Chlorohydrin. *J. Org. Chem.* **44**, 1716–1717 (1979).
30. McBee, J. K., Van Hooser, J. P., Jang, G. F. & Palczewski, K. Isomerization of 11-cis-Retinoids to All-trans-retinoids in Vitro and in Vivo. *J. Biol. Chem.* **276**, 48483–48493 (2001).
31. Kojima, R. *et al.* In vivo isomerization of retinoic acids. Rapid isomer exchange and gene expression. *J. Biol. Chem.* **269**, 32700–32707 (1994).
32. Van Rooden, E. J. *et al.* Mapping in vivo target interaction profiles of covalent inhibitors using chemical proteomics with label-free quantification. *Nat. Protoc.* **13**, 752–767 (2018).
33. Rappsilber, J., Mann, M. & Ishihama, Y. Protocol for micro-purification, enrichment, pre-fractionation and storage of peptides for proteomics using StageTips. *Nat. Protoc.* **2**, 1896–1906 (2007).
34. Distler, U., Kuharev, J., Navarro, P. & Tenzer, S. Label-free quantification in ion mobility–enhanced data-independent acquisition proteomics. *Nat. Protoc.* **11**, 795–812 (2016).
35. Distler, U. *et al.* Drift time-specific collision energies enable deep-coverage data-independent acquisition proteomics. *Nat. Methods* **11**, 167–170 (2014).
36. Kuharev, J., Navarro, P., Distler, U., Jahn, O. & Tenzer, S. In-depth evaluation of software tools for data-independent acquisition based label-free quantification. *Proteomics* **15**, 3140–3151 (2015).